



OPEN

Microglia contribute to the propagation of A β into unaffected brain tissue

Paolo d'Errico^{1,2}, Stephanie Ziegler-Waldkirch^{1,2}, Vanessa Aires^{1,3}, Philippe Hoffmann^{1,2}, Charlotte Mezö^{3,4}, Daniel Erny^{5,6,7}, Laura Sebastian Monasor⁶, Sabine Liebscher^{7,8,9}, Vidhya M. Ravi^{10,11,12,13}, Kevin Joseph^{10,11,13}, Oliver Schnell^{10,11,13}, Katrin Kierdorf^{14,15}, Ori Staszewski^{2,4,5}, Sabina Tahirovic⁶, Marco Prinz¹⁶ and Melanie Meyer-Luehmann^{1,2,15} ✉

Microglia appear activated in the vicinity of amyloid beta (A β) plaques, but whether microglia contribute to A β propagation into unaffected brain regions remains unknown. Using transplantation of wild-type (WT) neurons, we show that A β enters WT grafts, and that this is accompanied by microglia infiltration. Manipulation of microglia function reduced A β deposition within grafts. Furthermore, in vivo imaging identified microglia as carriers of A β pathology in previously unaffected tissue. Our data thus argue for a hitherto unexplored mechanism of A β propagation.

The aggregation of A β is an essential early trigger in Alzheimer's disease (AD) pathogenesis that leads to neurofibrillary tangles, neuronal dysfunction and dementia¹. Several cell types have been proposed to be causally involved in amyloid plaque formation, including microglia, owing to their close association with A β plaques^{2–4}. As soon as A β plaques form in the brain, microglia establish an intimate contact with them and become reactive^{5,6}. Those activated microglia have been linked to plaque growth by A β uptake followed by microglial cell death^{7,8}. Our group and others have recently implicated microglia in A β seeding^{9–11}, yet their role in propagating A β pathology remains elusive.

In support of the 'pathogenic spread' hypothesis¹², previous transplantation experiments showed that A β derived from transgenic host tissue is able to invade and deposit in non-transgenic grafts, leading to neurodegeneration^{13–15}. However, the mechanism by which A β spreads into the WT grafts is unknown, and a cell-mediated mechanism has not been proven so far.

In this study, we transplanted embryonic neuronal cells from WT mice into the neocortex of young, pre-depositing 5xFAD transgenic mice, confirming transplant integration into the host tissue as well as the survival of the grafts over several months (Fig. 1a,b and Extended Data Fig. 1a,b)¹³. As soon as 4 weeks after transplantation, A β plaques were present within WT grafts, and they increased over time (Fig. 1a and Extended Data Fig. 1a–c, yellow arrowheads). We first hypothesized that APP/A β is anterogradely transported

from the host transgenic neurons into the WT grafts, and we used *Thy1-GFP/5xFAD* mice as recipients to visualize the alignment of processes from the host mouse. Although we found a few fibers that crossed the host–graft boundary, most of the green fluorescent protein (GFP)-positive cells did not penetrate into the WT graft (Fig. 1b and Extended Data Fig. 1a,b), indicating that axonal transport is not likely to be involved in the propagation of A β pathology into WT grafts. The greatest amyloid accumulation manifested along the border, an area known to have a slightly higher microglia density. Therefore, we investigated whether, indeed, host microglia are able to invade the WT graft by using *Cx3cr1^{+/−}/5xFAD* mice. By 2 weeks after transplantation, massive invasion of CX3CR1-positive cells into the graft was evident, probably owing to injury or the placement of the graft itself, with the highest number of cells at the edges (Fig. 1c). This microglia accumulation ceased over time (Fig. 1d), although there was no prominent cell death (Fig. 1e,f). We observed many small A β particles within the cells or intimately associated with microglia (Extended Data Fig. 1d–f). Next, we characterized the cellular composition of the graft and confirmed the presence of doublecortin (DCX) in cellular samples, whereas we did not observe any signal for GFAP or IBA1 (Extended Data Fig. 2a). Furthermore, we detected NeuN-positive neurons at 4 and 16 weeks after transplantation as well as CX3CR1-positive microglia that were all double-labeled with IBA1 (Extended Data Fig. 2b–d). To prove that the microglia were indeed host-derived and not donor-derived, we transplanted embryonic cell suspensions from *Cx3cr1-GFP* mice into *Hexb^{tdTomato}* recipients that express tdTomato exclusively in resident microglia in the central nervous system¹⁶. No GFP-positive donor-derived cells could be detected in the graft, excluding microglia contamination from the donors (Extended Data Fig. 2e). To rule out a contribution of infiltrating monocytes from the periphery, we used *Ccr2^{−/−}/5xFAD* mice as recipients, which had similar A β load within the grafts when compared to *Ccr2^{+/−}/5xFAD* mice, despite having significantly fewer IBA1-positive cells (Extended Data Fig. 3a–c). Likewise, the number of microglia within grafts placed

¹Department of Neurology, Medical Center – University of Freiburg, Freiburg, Germany. ²Faculty of Medicine, University of Freiburg, Freiburg, Germany.

³Faculty of Biology, University of Freiburg, Freiburg, Germany. ⁴Institute of Neuropathology, Faculty of Medicine, University of Freiburg, Freiburg, Germany.

⁵Berta-Ottenstein-Programme, Faculty of Medicine, University of Freiburg, Freiburg, Germany. ⁶German Center for Neurodegenerative Diseases

(DZNE), Munich, Germany. ⁷Munich Cluster for Systems Neurology (SyNergy), Munich, Germany. ⁸Institute of Clinical Neuroimmunology, Klinikum der Universität München, Ludwig-Maximilians University Munich, Martinsried, Germany. ⁹Biomedical Center, Medical Faculty, Ludwig-Maximilians University Munich, Martinsried, Germany. ¹⁰Microenvironment and Immunology Research Laboratory, Medical Center – University of Freiburg, Freiburg, Germany.

¹¹Department of Neurosurgery, Medical Center – University of Freiburg, Freiburg, Germany. ¹²Neuroelectronic Systems, Medical Center – University of Freiburg, Freiburg, Germany. ¹³Translational NeuroOncology Research Group, Medical Center – University of Freiburg, Freiburg, Germany. ¹⁴Centre for Integrative Biological Signalling Studies, University of Freiburg, Freiburg, Germany. ¹⁵Center for Basics in NeuroModulation (NeuroModulBasics), Faculty of Medicine, University of Freiburg, Freiburg, Germany. ¹⁶Signalling Research Centres BLOSS and CIBSS, University of Freiburg, Freiburg, Germany.

✉e-mail: melanie.meyer-luehmann@uniklinik-freiburg.de

either in *Cx3cr1^{+/-}/5xFAD* or *Hexb^{tdTomato}/5xFAD* recipients was similar (Extended Data Fig. 3d,e), confirming that resident microglia rather than peripheral monocytes from the hosts were infiltrating the grafts. Microglia within the grafts displayed the typical arborization with fine delineated processes similar to non-plaque-associated microglia outside the grafts (Fig. 1g), and the number of microglia surrounding amyloid plaques increased with plaque size independent of their graft or host association (Fig. 1h). By performing bulk RNA sequencing (RNA-seq) of fluorescence-activated cell-sorted (FACS) microglia derived from within or outside the grafts, we identified only three differentially expressed genes out of 15,548 genes (Fig. 1i and Supplementary Fig. 1), indicating that host microglia maintain their transcriptome after migration to the graft and reaffirming that microglia in both compartments are similar.

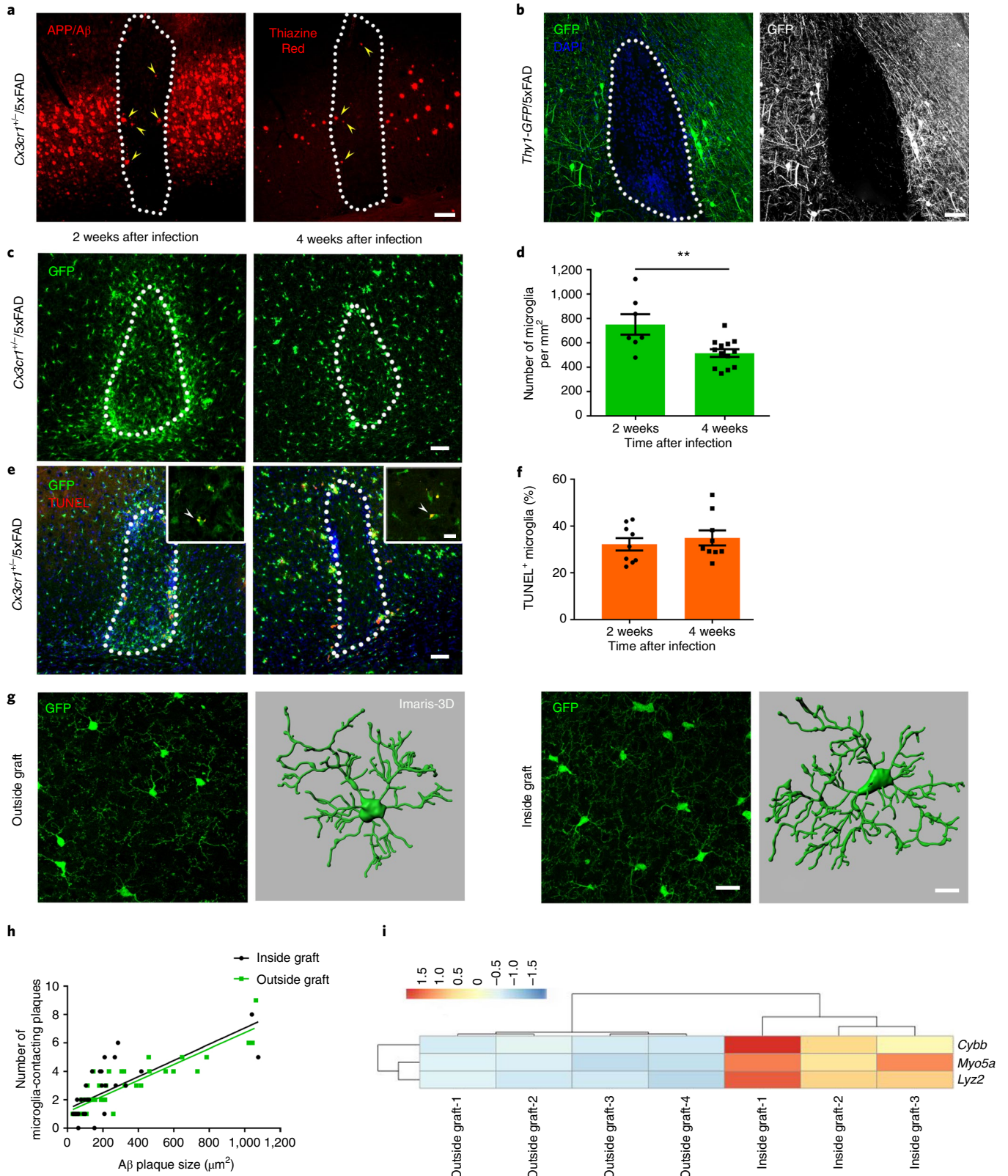
The fact that microglia are phagocytic cells and, as shown, invade the graft prompted us to speculate that microglia take up A β from the recipient tissue and invade the WT graft, where A β finally deposits. Manipulating microglial function should, therefore, alter this process. Because the capacity of microglia to phagocytose A β is compromised in the aging brain and AD¹⁷⁻²⁰, we performed in vitro experiments to compare the amount of A β incorporated by microglia of adult and old 5xFAD mice (Extended Data Fig. 4a). Both the percentage of A β -containing microglia and the number of A β puncta per cell were significantly decreased in old mice (Extended Data Fig. 4b-d). Next, we analyzed the phagocytic capacity of microglia in vivo after administration of methoxy-XO4. Flow cytometric analysis of microglia from adult and old WT and 5xFAD mice (Extended Data Fig. 4e and Supplementary Fig. 2) showed a significantly higher percentage of methoxy-XO4-positive microglia in old compared to adult animals (Extended Data Fig. 4f), whereas mean fluorescence intensity (MFI) of methoxy-XO4 was significantly decreased in microglia from old 5xFAD mice (Extended Data Fig. 4g). These data confirmed a decline in microglial phagocytosis of A β in old 5xFAD mice. Finally, we used young or old *Cx3cr1^{+/-}/5xFAD* mice as recipients and compared the amyloid load inside the grafts 4 weeks later. The amount of A β within the grafts of old mice was strongly reduced, even though microglia density was equivalent (Extended Data Fig. 4h-j), suggesting that compromised phagocytosis by aged microglia in the transgenic host tissue subsequently lead to a decrease in amyloid deposition in WT grafts. We validated our hypothesis further by using *Cx3cr1*-deficient 5xFAD transgenic mice as recipients. In accordance with the higher A β clearance propensity in mice lacking CX3CR1 (ref. ²¹), the amyloid load was again significantly reduced in the grafts, although the number of microglia in both genotypes was similar (Extended Data Fig. 5a-c). Next we took advantage of *Irf8^{-/-}/Cx3cr1^{+/-}* transgenic mice, which are characterized by microglia with reduced and swollen processes^{22,23} and reduced motility²⁴. Indeed, IRF8-deficient microglia exhibited morphological alterations, such as reduced and shorter branches

(Fig. 2a)²². Under steady-state conditions, microglial process motility in *Irf8^{-/-}* mice was strongly impaired (Supplementary Videos 1 and 2). Furthermore, focal-laser-induced damage followed by time lapse in vivo two-photon imaging revealed a diminished microglia response to the lesion in *Irf8^{-/-}* mice (Supplementary Videos 3 and 4 and Fig. 2b). Quantification of responding cells based on their distance from the injury site identified significantly fewer responding cells in *Irf8^{-/-}* mice than in control groups (Fig. 2c). In contrast to the cell bodies, which remained at their original positions^{25,26}, the speed of microglial processes and the distance to the injury declined markedly in these mice (Fig. 2d,e). We then generated *Irf8^{-/-}/Cx3cr1^{+/-}/5xFAD* mice, which had similar numbers of A β plaques (Extended Data Fig. 6a-d) with significantly less microglial clustering around A β plaques and a smaller amount of internalized A β (Extended Data Fig. 6e-h). Notably, microglia failed to migrate into the WT grafts, and, thus, the number of microglia that entered the grafts was substantially reduced, resulting in a reduction in amyloid deposits in the grafts (Fig. 2f-h), further corroborating our hypothesis. Strikingly, we also found evidence for microglia propagating A β into WT tissue by depleting microglia using the colony-stimulating factor 1 receptor (CSF-1R) inhibitor BLZ945 in *Cx3cr1^{+/-}/5xFAD* recipient mice (Extended Data Fig. 7a). We obtained an approximately 80% cell reduction in the cortex of mice treated with the CSF-1R inhibitor as well as within the grafts (Extended Data Fig. 7b-f), resulting, again, in significantly fewer A β deposits within the grafts (Extended Data Fig. 7e,g). Because the elimination of microglia did not completely prevent A β plaque formation within the grafts, we cannot rule out the possibility that additional factors (for example, diffusion) at least partially contribute to this propagation process. Neither CSF-1R inhibitor treatment nor IRF8 deficiency had an effect on the presence of astrocytes within the grafts, despite lowered amyloid content (Extended Data Fig. 8a-d), indicating that astrocytes might play only a minor role in amyloid propagation, at least in our grafting model system. To finally demonstrate the active involvement of microglia in A β propagation into grafts, we performed repetitive two-photon in vivo imaging of *Irf8^{+/+}/Cx3cr1^{+/-}/5xFAD* mice in comparison to *Irf8^{-/-}/Cx3cr1^{+/-}/5xFAD* mice and examined microglial motility associated with A β transport in response to a laser-induced focal tissue injury. Microglia moved to the lesion site, where A β plaques started to build up concomitantly (Fig. 3a,c,d,e) owing to microglial transport of A β toward the lesion site (Supplementary Videos 5 and 6). By contrast, movement of A β -laden microglia toward the lesion site was not evident in *Irf8^{-/-}/Cx3cr1^{+/-}/5xFAD* mice (Fig. 3b). We further validated our findings in the absence of tissue injury by co-culturing young brain slices from WT animals with old *Cx3cr1^{+/-}/5xFAD* brain slices, as recently reported²⁰. We detected at 14 days in vitro many GFP-positive microglia migrating toward the WT tissue, with fewer cells reaching the edges of the young

Fig. 1 | Characteristics of microglia in neuronal WT grafts. **a**, Fluorescence microscopy of a graft 4 weeks after injection into *Cx3cr1^{+/-}/5xFAD* cortex. Yellow arrowheads indicate A β deposition (left: 6E10 in red, from $n=9$ mice; right: Thiazine Red in red, from $n=4$ mice) inside the graft (outlined with a white dotted line). Scale bar, 50 μ m. **b**, Representative fluorescence microscopy of a graft at 4 weeks after injection in *Thy1-GFP/5xFAD* recipient mice, from $n=4$ mice. Scale bar, 50 μ m. **c**, Analysis of microglia accumulation inside grafts at 2 and 4 weeks after injection in *Cx3cr1^{+/-}/5xFAD* transgenic mice. Scale bar, 50 μ m. **d**, Graph shows mean (\pm s.e.m.) of microglia cell density inside grafts; each symbol represents one graft from $n=7$ (2 weeks) and $n=13$ (4 weeks) mice. Significant differences were determined using the Mann-Whitney test ($**P=0.0085$). **e**, Fluorescence microscopy of TUNEL-positive (red) microglia (green) inside grafts at 2 and 4 weeks after injection in *Cx3cr1^{+/-}/5xFAD* transgenic mice. Scale bars, 50 μ m in the overview and 15 μ m in the inset. **f**, Percentage of TUNEL-positive microglia inside grafts. Each symbol represents one graft from $n=9$ mice per group. Data are presented as mean (\pm s.e.m.). Significant differences were determined using the two-tailed Mann-Whitney test. **g**, Confocal microscopy and Imaris-3D reconstruction of microglia outside (left) or inside (right) the graft. Scale bars, 20 μ m in the confocal acquisition and 10 μ m in the Imaris reconstruction. For 3D reconstruction, we considered two regions inside and outside grafts in $n=2$ mice per group. **h**, Pearson correlation between the number of microglia-contacting plaques and plaque size inside ($r=0.53$, $P<0.0001$) and outside ($r=0.80$, $P<0.0001$) the grafts. Each symbol represents one compact plaque from $n=7$ *Cx3cr1^{+/-}/5xFAD* mice. **i**, Heat map of the three top differentially regulated genes ($**P<0.01$) in microglia FACS-sorted from either isolated cortical grafts or cortical regions outside the transplant that were used as controls. Differentially expressed genes were determined using the limma-voom package in R.

tissue and only some that migrated deeper into the tissue (Extended Data Fig. 9a,c). Upon closer inspection, we noticed A β -containing microglia clearly migrating from the old *Cx3cr1*^{+/-}/5xFAD brain slice to the young WT slice (Extended Data Fig. 9b,d), confirming the notion that A β is transported by microglia into non-diseased brain tissue.

Together, these findings highlight the importance of microglia for the propagation of A β pathology into WT grafts by acting as A β carriers that migrate toward previously unaffected brain tissue. By using neural grafting experiments in 5xFAD mice with altered microglial function, we propose that the formation of A β plaques in grafted, unaffected tissue is, at least to some extent, dependent on host



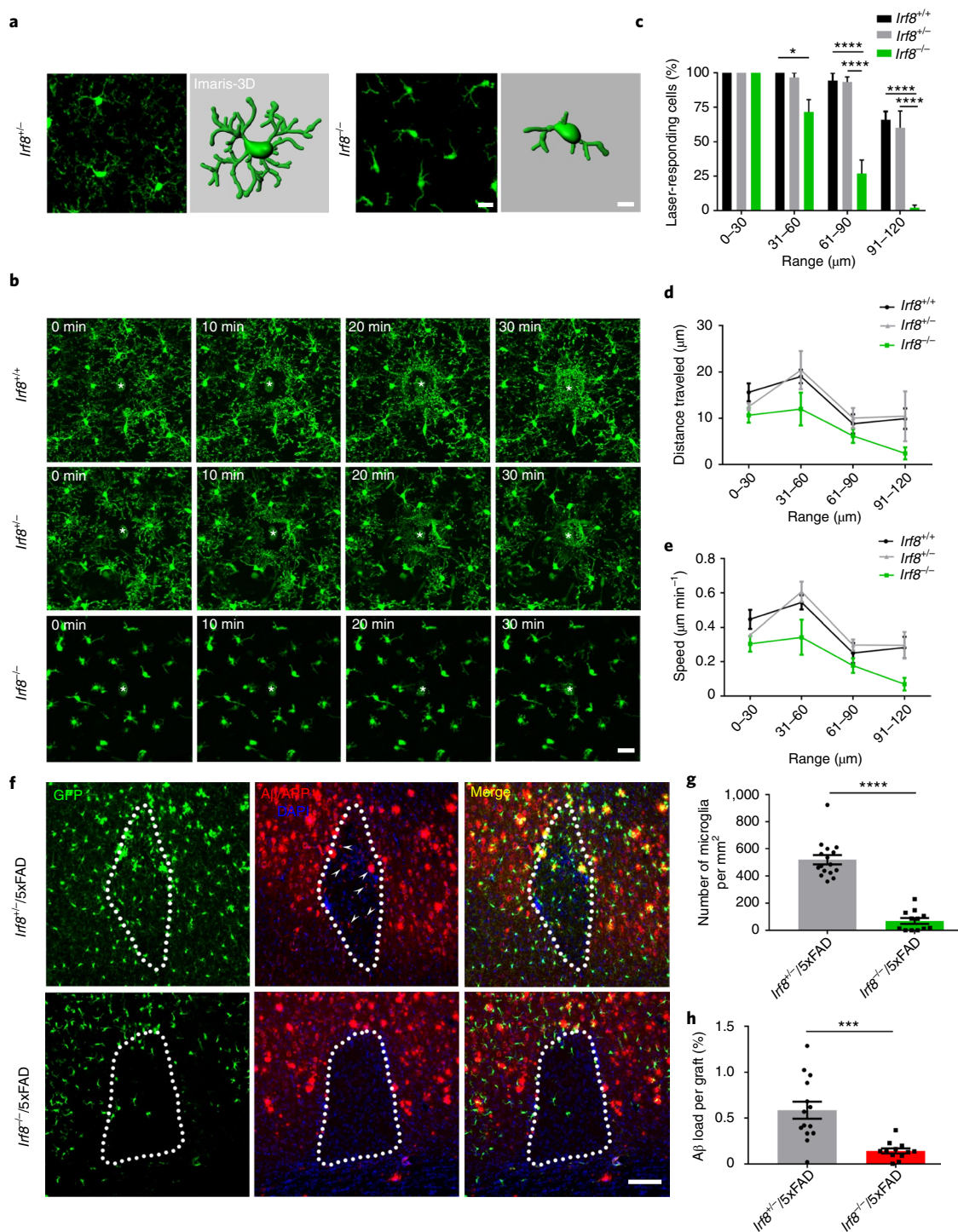


Fig. 2 | Decreased A β deposition inside grafts in *Irf8*^{-/-}/5xFAD recipient mice. **a, Representative confocal images (left) and corresponding Imaris-3D reconstruction (right) of microglia in the cortex of *Irf8*^{+/+} and *Irf8*^{-/-} mice. Scale bars, 15 μ m in the left image and 10 μ m in the 3D reconstruction on the right. For 3D reconstruction, two cells were considered in $n = 2$ mice per group. **b–e**, In vivo two-photon analysis of microglia process motility between 0 and 30 min after laser lesion ablation in *Irf8*^{+/+}, *Irf8*^{+/-} and *Irf8*^{-/-} mice. Scale bar, 20 μ m. Quantification of percentage of laser-responding cells (**c**), mean distance traveled (**d**) and speed of microglia processes (**e**) based on their distance from the injury site. Data are presented as mean (\pm s.e.m.). Significant differences were determined using two-way ANOVA followed by Sidak's multiple comparison test (in **c**, **** $P < 0.0001$ and * $P = 0.030$), Tukey's multiple comparison test $F_{6,46} = 0.8661$ (in **d**, range 31–60 μ m: * $P = 0.044$ *Irf8*^{+/+} versus *Irf8*^{-/-} and ** $P = 0.008$ *Irf8*^{+/-} versus *Irf8*^{-/-}; range 91–120 μ m: $P = 0.054$ *Irf8*^{+/+} versus *Irf8*^{-/-} and * $P = 0.0199$ *Irf8*^{+/-} versus *Irf8*^{-/-}) and Tukey's multiple comparison test $F_{6,46} = 0.9551$ (in **e**, range 31–60 μ m: * $P = 0.0484$ *Irf8*^{+/+} versus *Irf8*^{-/-} and ** $P = 0.0039$ *Irf8*^{+/-} versus *Irf8*^{-/-}; range 91–120 μ m: $P = 0.0584$ *Irf8*^{+/+} versus *Irf8*^{-/-} and * $P = 0.0235$ *Irf8*^{+/-} versus *Irf8*^{-/-}). Data are from $n = 4$ *Irf8*^{+/+}, $n = 5$ *Irf8*^{+/-} and $n = 6$ *Irf8*^{-/-} mice. **f**, Grafts in *Irf8*^{+/+}/5xFAD and *Irf8*^{-/-}/5xFAD recipient mice immunostained for A β (6E10, red; white arrowheads indicate A β depositions) and DAPI (blue). Scale bar, 100 μ m. **g, h**, Graphs show mean (\pm s.e.m.) microglia density (**g**) and percentage of A β inside the grafts (**h**) in the two groups of mice. Each symbol represents one graft from $n = 7$ *Irf8*^{+/+}/5xFAD and $n = 6$ *Irf8*^{-/-}/5xFAD mice. Significant differences were determined using the two-tailed Mann-Whitney test (**** $P < 0.0001$ in **g** and *** $P = 0.001$ in **h**).**

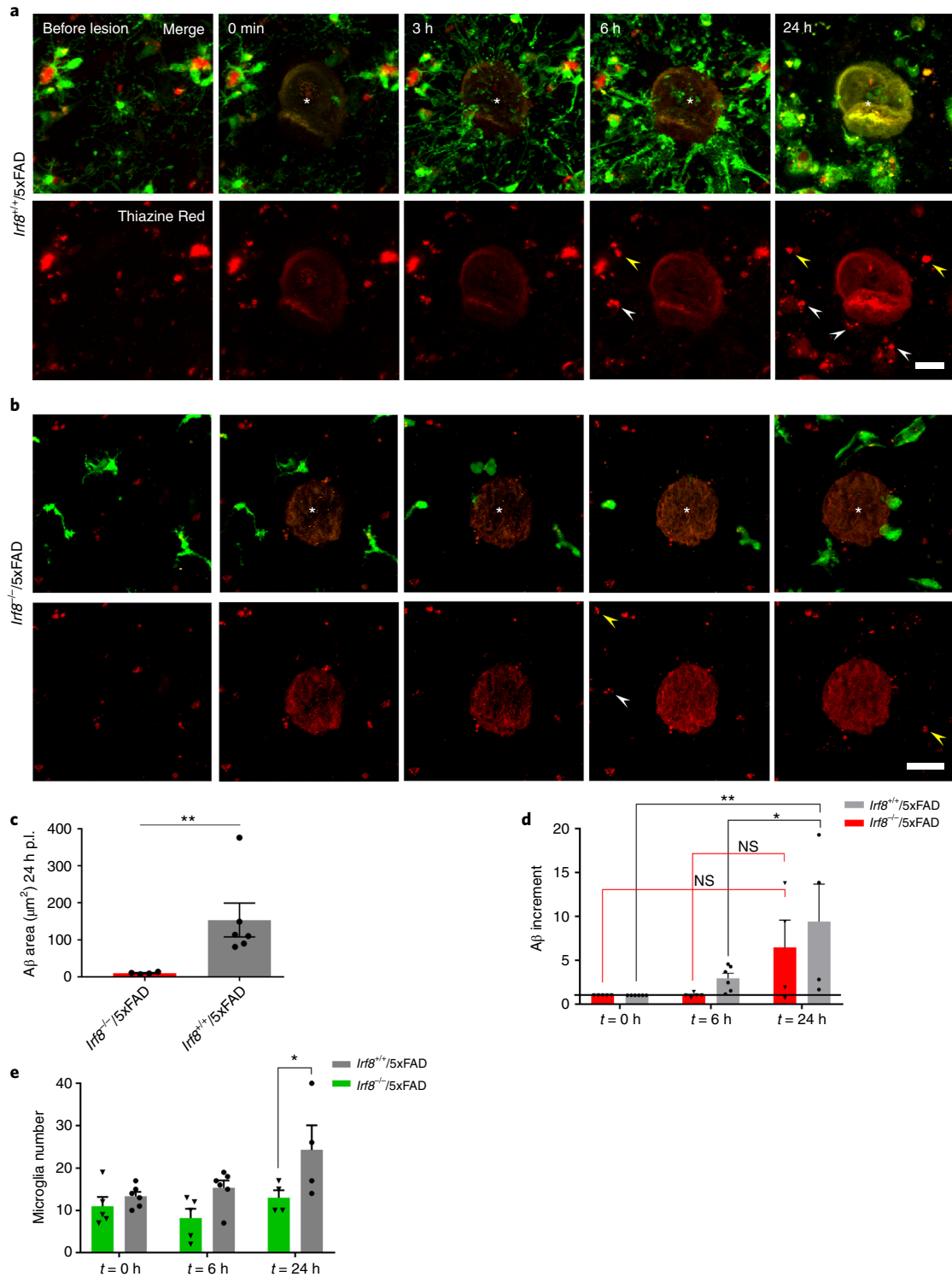


Fig. 3 | In vivo two-photon imaging of Aβ-containing microglia movement after laser lesion. a, b, In vivo two-photon imaging of Aβ-containing microglial responses at different time points after laser-induced tissue injury in *Irf8*^{+/+}/*Cx3cr1*^{+/-}/5xFAD mice (**a**) and *Irf8*^{-/-}/*Cx3cr1*^{+/-}/5xFAD mice (**b**). The top panels show merged images of GFP (green) and Thiazine Red (red) signal; the bottom panel shows only the Thiazine Red signal; asterisks indicate laser ablations; white arrowheads depict internalized Aβ moving with time; and yellow arrowheads indicate amyloid material associated with small microglia debris or no microglia association at all (shown only in the red channel). Scale bars, 50 μm. **c–e**, Graphs show mean (± s.e.m.) of Aβ accumulation at the lesion site 24 h post lesion (p.l.) in both groups of mice (**c**), relative increment of Aβ at the lesion site at 0, 6 and 24 h p.l. (**d**), and microglia accumulation at 0, 6 and 24 h p.l. (**e**). Each symbol represents one laser lesion from *n* = 6 *Irf8*^{+/+}/*Cx3cr1*^{+/-}/5xFAD mice and *n* = 5 *Irf8*^{-/-}/*Cx3cr1*^{+/-}/5xFAD mice. Significant differences were determined using either the two-tailed Mann–Whitney test (***P* = 0.0095 in **c**) or two-way ANOVA with Sidak’s multiple comparison test (**P* = 0.0436 and ***P* = 0.0068 in **d** and **P* = 0.0282 in **e**). NS, not significant.

microglia functionality (Supplementary Fig. 3). Although our findings need to be repeated in a physiologically more relevant context, one can envision that physical trauma, traumatic brain injury, stroke, tumor or neurodegeneration might become the trigger for microglia migration and transport of A β . We conclude that targeting microglia function might provide an opportunity to interfere with the propagation of A β .

Online content

Any methods, additional references, Nature Research reporting summaries, source data, extended data, supplementary information, acknowledgements, peer review information; details of author contributions and competing interests; and statements of data and code availability are available at <https://doi.org/10.1038/s41593-021-00951-0>.

Received: 4 March 2021; Accepted: 30 September 2021;
Published online: 22 November 2021

References

- Selkoe, D. J. & Hardy, J. The amyloid hypothesis of Alzheimer's disease at 25 years. *EMBO Mol. Med.* **8**, 595–608 (2016).
- Sosna, J. et al. Early long-term administration of the CSF1R inhibitor PLX3397 ablates microglia and reduces accumulation of intraneuronal amyloid, neuritic plaque deposition and pre-fibrillar oligomers in 5XFAD mouse model of Alzheimer's disease. *Mol. Neurodegener.* **13**, 11 (2018).
- Spangenberg, E. et al. Sustained microglial depletion with CSF1R inhibitor impairs parenchymal plaque development in an Alzheimer's disease model. *Nat. Commun.* **10**, 3758 (2019).
- Spangenberg, E. E. et al. Eliminating microglia in Alzheimer's mice prevents neuronal loss without modulating amyloid- β pathology. *Brain J. Neurol.* **139**, 1265–1281 (2016).
- Meyer-Luehmann, M. et al. Rapid appearance and local toxicity of amyloid- β plaques in a mouse model of Alzheimer's disease. *Nature* **451**, 720–724 (2008).
- Prinz, M., Jung, S. & Priller, J. Microglia biology: one century of evolving concepts. *Cell* **179**, 292–311 (2019).
- Baik, S. H., Kang, S., Son, S. M. & Mook-Jung, I. Microglia contributes to plaque growth by cell death due to uptake of amyloid β in the brain of Alzheimer's disease mouse model. *Glia* **64**, 2274–2290 (2016).
- Mildner, A. et al. Distinct and non-redundant roles of microglia and myeloid subsets in mouse models of Alzheimer's disease. *J. Neurosci.* **31**, 11159–11171 (2011).
- Venegas, C. et al. Microglia-derived ASC specks cross-seed amyloid- β in Alzheimer's disease. *Nature* **552**, 355–361 (2017).
- Ziegler-Waldkirch, S. et al. Seed-induced A β deposition is modulated by microglia under environmental enrichment in a mouse model of Alzheimer's disease. *EMBO J.* **37**, 167–182 (2018).
- Parhizkar, S. et al. Loss of TREM2 function increases amyloid seeding but reduces plaque-associated ApoE. *Nat. Neurosci.* **22**, 191–204 (2019).
- Walsh, D. M. & Selkoe, D. J. A critical appraisal of the pathogenic protein spread hypothesis of neurodegeneration. *Nat. Rev. Neurosci.* **17**, 251–260 (2016).
- Meyer-Luehmann, M. et al. Extracellular amyloid formation and associated pathology in neural grafts. *Nat. Neurosci.* **6**, 370–377 (2003).
- Bachhuber, T. et al. Inhibition of amyloid- β plaque formation by α -synuclein. *Nat. Med.* **21**, 802–807 (2015).
- Espuny-Camacho, I. et al. Hallmarks of Alzheimer's disease in stem-cell-derived human neurons transplanted into mouse brain. *Neuron* **93**, 1066–1081.e8 (2017).
- Masuda, T. et al. Novel Hexb-based tools for studying microglia in the CNS. *Nat. Immunol.* **21**, 802–815 (2020).
- Floden, A. M. & Combs, C. K. Microglia demonstrate age-dependent interaction with amyloid- β fibrils. *J. Alzheimers Dis.* **25**, 279–293 (2011).
- Krabbe, G. et al. Functional impairment of microglia coincides with beta-amyloid deposition in mice with Alzheimer-like pathology. *PLoS ONE* **8**, e60921 (2013).
- Sebastian Monasor, L. et al. Fibrillar A β triggers microglial proteome alterations and dysfunction in Alzheimer mouse models. *eLife* **9**, e54083 (2020).
- Daria, A. et al. Young microglia restore amyloid plaque clearance of aged microglia. *EMBO J.* **36**, 583–603 (2017).
- Liu, Z., Condello, C., Schain, A., Harb, R. & Grutzendler, J. CX3CR1 in microglia regulates brain amyloid deposition through selective protofibrillar amyloid- β phagocytosis. *J. Neurosci.* **30**, 17091–17101 (2010).
- Hagemeyer, N. et al. Transcriptome-based profiling of yolk sac-derived macrophages reveals a role for Irf8 in macrophage maturation. *EMBO J.* **35**, 1730–1744 (2016).
- Kierdorf, K. et al. Microglia emerge from erythromyeloid precursors via Pu.1- and Irf8-dependent pathways. *Nat. Neurosci.* **16**, 273–280 (2013).
- Masuda, T. et al. IRF8 is a transcriptional determinant for microglial motility. *Purinergic Signal.* **10**, 515–521 (2014).
- Davalos, D. et al. ATP mediates rapid microglial response to local brain injury in vivo. *Nat. Neurosci.* **8**, 752–758 (2005).
- Nimmerjahn, A., Kirchhoff, F. & Helmchen, F. Resting microglial cells are highly dynamic surveillants of brain parenchyma in vivo. *Science* **308**, 1314–1318 (2005).

Publisher's note Springer Nature remains neutral with regard to jurisdictional claims in published maps and institutional affiliations.



Open Access This article is licensed under a Creative Commons Attribution 4.0 International License, which permits use, sharing, adaptation, distribution and reproduction in any medium or format, as long as you give appropriate credit to the original author(s) and the source, provide a link to the Creative Commons license, and indicate if changes were made. The images or other third party material in this article are included in the article's Creative Commons license, unless indicated otherwise in a credit line to the material. If material is not included in the article's Creative Commons license and your intended use is not permitted by statutory regulation or exceeds the permitted use, you will need to obtain permission directly from the copyright holder. To view a copy of this license, visit <http://creativecommons.org/licenses/by/4.0/>.

© The Author(s) 2021

Methods

Animals. To visualize neuronal structures, *Thy1-eGFP* mice²⁷ were crossed with 5xFAD transgenic mice co-expressing human APP^{K670N/M671L(Sw)+1716V(FE)+V717I(Lo)} and PS1^{M146L+L286V} under the control of the neuron-specific *Thy1* promoter²⁸. To visualize green fluorescence in microglia, we intercrossed *Cx3cr1^{GFP/wt}/5xFAD* (here reported as *Cx3cr1^{+/+}/5xFAD*)²⁹ mice to obtain *Cx3cr1^{+/+}/5xFAD* or *Cx3cr1^{-/-}/5xFAD*; to visualize red fluorescence in microglia, we crossed *Hexb^{tdTomato}* with 5xFAD mice and obtained homozygous *Hexb^{tdTomato}/5xFAD* mice. We backcrossed 5xFAD with *Irf8^{-/-}/Cx3cr1^{GFP/GFP}* mice (courtesy of Clemens Lange) to obtain *Irf8^{+/+}/Cx3cr1^{+/+}/5xFAD*, *Irf8^{+/+}/Cx3cr1^{-/-}/5xFAD* or *Irf8^{-/-}/Cx3cr1^{+/+}/5xFAD* mice. The *Hexb^{tdTomato}* and *Ccr2^{-/-}/5xFAD* transgenic mice were kindly provided by Marco Prinz. All mice were on a C57BL/6 background. For this study, only female mice were used, to minimize variability and reduce sample size. Animals were group-housed under specific pathogen-free conditions and kept under a 12-h light–dark cycle with food and water ad libitum at a temperature of 22 °C and 73% humidity. For all experiments, mice were randomly allocated into each experimental group. All animal experiments were carried out in accordance with the policies of the State of Baden-Württemberg under license number G16-100.

Preparation of cortical cell suspensions for intracerebral grafting. Primary cortical neurons were isolated from C57BL/6 WT mice at embryonic day 16–17. Cortices were dissected on ice, trypsinized for 10 min with 0.05% Trypsin-EDTA (Gibco) at 37 °C and washed three times in HBSS (Gibco). Cells were triturated in DMEM (Gibco) by pipetting up and down until the suspension was homogenous and maintained on ice until the injection.

Intracerebral grafting. Mice were anesthetized via intraperitoneal (i.p.) injection with a mixture of ketamine (100 mg kg⁻¹ body weight) and xylazine (10 mg kg⁻¹ body weight) dissolved in saline. For bilateral stereotaxic transplantation of neuronal cell suspensions, a Hamilton syringe was placed into the cortex (AP +1.8 mm, L ±1.5 mm, DV -1.3 mm) of 9–10-week-old (young adult) or 8–11-month-old (adult) mice. Animals were injected with 3 µl (approximately 20,000 cells) per hemisphere at an injection speed of 1 µl min⁻¹. After each injection, the needle was kept in place for 1 min before it was slowly withdrawn. The surgical site was cleaned with sterile saline and the incision sutured. Mice were monitored until recovery from anesthesia and followed for 2, 4 or 16 weeks.

Isolation of primary microglia for in vitro culture. The whole brain from adult (20–30-week-old) or old (50–60-week-old) mice was isolated after transcardial perfusion with 1× PBS, and a single-cell suspension was prepared. The homogenate was filtered through a cell strainer (70 µm) and separated by 37% Percoll gradient centrifugation at 400g for 30 min at 4 °C. The myeloid-containing phase was collected and washed once with HBSS. The cells were resuspended in culture medium (DMEM/F-12, 1× penicillin–streptomycin, 10% FCS) and plated onto poly-lysinated coverslips for 24 h at 37 °C and 5% CO₂. The cells were quickly washed with 1× PBS and fixed with 4% paraformaldehyde (PFA) for 15 min. Microglia were isolated from 3–6 animals per group.

Histology and immunocytochemistry. Mice were overdosed with an i.p. injection of ketamine and xylazine and transcardially perfused with 10 ml of ice-cold PBS followed by 10 ml of ice-cold 4% PFA (ROTI-Histofix, Carl Roth) in PBS. Brains were isolated and post-fixed in 4% PFA for 24 h at 4 °C, followed by incubation in 30% sucrose (in PBS, pH 7.5) for 48 h. Frozen brains were cut into 25 µm-thick coronal sections on a sliding microtome (SM2000R, Leica Biosystems) and collected in 15% glycerol dissolved in PBS. Sections were incubated overnight at 4 °C with the following antibodies diluted in 1× PBS containing 5% normal goat serum (NGS) and 0.5% Triton X-100: anti-IBA1 (rabbit, 1:500, Abcam, ab178846), anti-GFAP (mouse, 1:500, Sigma-Aldrich, GA5), anti-Aβ (mouse, 1:1,000, Covance, 6E10) and anti-NeuN (mouse, 1:500, Abcam). Appropriate secondary antibodies conjugated to Alexa Fluor 488 or 555 (1:1,000) were used before counterstaining with DAPI (1:10,000).

Primary microglia cultures were immunolabeled using anti-Aβ (mouse, 1:1,000, Covance, 6E10) and anti-IBA1 (rabbit, 1:1,000, Wako, 019-19741) diluted in 1× PBS containing 5% NGS overnight at 4 °C and incubated for 1.5 h with secondary antibodies conjugated to Alexa Fluor 488 or 555 (1:1,000) and finally counterstained with DAPI (1:10,000).

TUNEL apoptosis assay. For the labeling of apoptotic cells inside grafts, the In Situ Cell Death Detection Kit (Roche) was used. This method is based on TUNEL. Sections were mounted on glass slides and dried overnight. The slides were post-fixed in 4% PFA for 10 min and washed for 20 min in PBS, followed by permeabilization in ice-cold 0.5% Triton X-100 and 0.1% sodium citrate for 2 min at 4 °C. The freshly prepared TUNEL reaction mixture was kept in the dark and on ice until use. The slides were incubated with 50 µl of TUNEL reaction mixture in a humid chamber for 1 h at 37 °C. After this incubation step, slides were washed three times for 5 min each in PBS, dried, and covered with mounting medium and a glass coverslip. Slides were kept in the dark at 4 °C until they were used for microscopy. As a positive control, sections were incubated with recombinant

DNAse I. For double labeling of TUNEL and antibodies, first, antibody labeling was done, followed by staining with the TUNEL kit.

Confocal images of the stained grafts were taken with an Olympus confocal microscope (FluoView FV 1000), and the percentage of TUNEL-positive microglial cells inside grafts was quantified using ImageJ (version 1.52a).

Microglia counting and assessment of Aβ. Every tenth brain section was immunohistochemically labeled with the 6E10 antibody specific to human Aβ/APP to easily identify the graft, as grafted WT cells are negative for APP, whereas the recipient surrounding tissue has a high content of intracellular APP staining. Fluorescence sections were imaged with a Zeiss fluorescence microscope (Axio Imager M2M) and opened with ImageJ for analysis. Total Aβ load in the graft was determined by calculating the per cent area fraction occupied by Aβ-positive staining in the graft, and the density of microglia inside the graft was counted manually. Each data point represents one graft in the histogram. Data were excluded if intracerebral grafting was unsuccessful or no graft was present.

Microglia depletion efficiency was determined by counting the number of GFP-positive microglia in the cortex of the CSF-1R- and vehicle-treated animals; 10–12 sections per animal were analyzed. Cell counting and the area of the cortex were measured with ImageJ, and the values were expressed as cell density (microglia per mm²).

To quantify the compact Aβ plaques in the cortex and hippocampus of *Irf8/5xFAD* mice, 5–6 brain sections per mouse were acquired with the Zeiss fluorescence microscope, and the number of Thiazine Red-positive plaques in the region of interest was counted manually with ImageJ.

For quantification of Aβ inside microglia of *Irf8/5xFAD* mice, three brain sections per mouse were acquired with an Olympus confocal microscope at ×20 magnification, and the amount of internalized Aβ was quantified using ImageJ.

For quantification of Aβ internalized by isolated microglia, immunolabeled cells were imaged with the Zeiss fluorescence microscope; the number of Aβ spots inside each cell and the percentage of Aβ-containing microglia were manually counted in ImageJ.

Immunoblot analysis of grafts. The cortical cell suspension was centrifuged at 800g for 5 min at 4 °C, and the pellet was lysed by resuspension in RIPA buffer (1 ml per 1 × 10⁷ cells). After 30-min incubation on ice, the samples were centrifuged at 13,000g for 10 min at 4 °C, and the supernatant was stored at -20 °C until use. Brain homogenate of a 12-month-old 5xFAD mouse was prepared as previously described¹⁰. The total protein concentration was determined using a Pierce BCA Protein Assay Kit (Thermo Fisher Scientific). For separation, samples were mixed with NuPAGE Sample Reducing Agent (10×) and NuPAGE LDS Sample Buffer (4×) and loaded onto NuPAGE 4–12% Bis-Tris Mini Gels (Invitrogen).

Proteins were transferred onto PVDF membranes (Bio-Rad) and incubated with specific antibodies against Aβ (mouse, 1:1,000, Covance, 6E10), DCX (rabbit, 1:2,000, Abcam, ab18723), GFAP (rabbit, 1:2,000, Dako, Z033401-2), IBA1 (rabbit, 1:100, Wako, 016-20001), α-tubulin (chicken, 1:1,000; Abcam, ab89984) and β-actin–HRP (mouse, 1:3,000, Abcam, ab20272) and incubated with the corresponding HRP-linked secondary antibodies. Clarity Western ECL Substrate (Bio-Rad) was used for protein visualization. The blot was acquired with Image Lab 4 software (Bio-Rad).

Laser lesion and in vivo imaging of microglia process outgrowth. Animals were anesthetized via i.p. injection of ketamine (100 mg kg⁻¹ body weight) and xylazine (10 mg kg⁻¹ body weight), and a 3-mm cranial window was implanted over the somato-sensory cortex of 12–14-week-old *Irf8^{+/+}*, *Irf8^{+/-}* and *Irf8^{-/-}* mice. During the imaging session, the body temperature was monitored and maintained at 36–37 °C using a heating blanket. Depth of anesthesia was assessed by monitoring pinch withdrawal and vibrissae movements.

Laser lesion and acute two-photon imaging were carried out using Olympus FV1000 with Mai Tai DeepSee Laser (Spectra-Physics) with an excitation wavelength of 900 nm and an emission filter of 515–560 nm. Focused laser injury was induced in a small area of about 80 µm² within the region of interest at 50 µm below the pial surface using a laser pulse (75% power for 30 s) with a frequency of 8 µs per pixel. Microglia response was recorded every 5 min for a total of 35 min at a depth of 30–70 µm with 2.5-µm *z* increments and 512 × 512-pixel resolution. In each mouse, 4–6 different sites were recorded. At the end of the experiment, mice were killed by decapitation.

Quantification of process microglia movement. The extension of individual microglia processes was tracked manually and measured using ImageJ considering the initial distance (at *t* = 0 min) and the final distance (at *t* = 35 min) from the center of the laser lesion. The mean speed and distance traveled were calculated for each microglial process. The percentage of responsive microglia cells was quantified by counting cells that showed at least one process moving toward the lesion site. The positions of the processes at *t* = 0 min were divided into four ranges: 0–30 µm, 31–60 µm, 61–90 µm and 91–120 µm (see the results above).

Laser lesion and in vivo imaging of Aβ-containing microglia in *Irf8^{+/+}/Cx3cr1^{+/+}/5xFAD* and *Irf8^{-/-}/Cx3cr1^{+/+}/5xFAD* mice. *Irf8^{+/+}/Cx3cr1^{+/+}/5xFAD* and *Irf8^{-/-}/Cx3cr1^{+/+}/5xFAD* mice (7–10 months old) were anesthetized via

i.p. injection of ketamine (100 mg kg⁻¹ body weight) and xylazine (10 mg kg⁻¹ body weight), and a craniotomy was performed as described above, but before covering the exposed cortex with the glass coverslip, the dura was carefully removed, and 10 µl of 0.01% Thiazine Red diluted in sterile 1× PBS was applied to the cerebral cortex for 5 min.

Laser lesion and acute two-photon imaging were carried out as described above with the following main differences: (1) laser injury was induced in a larger area of about 2 mm² within the region of interest; (2) emission filters of 590–650 nm and 515–560 nm were used to detect, respectively, Thiazine Red and GFP signal; and (3) microglia response was recorded every hour for a total of 6 h on the first day at a depth of 0–70 µm. Imaging of the same lesioned region was carried out, as a single acquisition, 24 h later. At the end of the experiment, the mouse was killed by decapitation.

Aβ area and microglia number were quantified, using ImageJ, after lesion induction (*t* = 0 h), at the end of the acute imaging session (*t* = 6 h) and after 24 h (*t* = 24 h) in a defined area of 150 µm × 150 µm around the lesion, to calculate the Aβ and microglia movement over time between the two groups.

In vivo Aβ phagocytosis assay. 5xFAD mice (young adults: 10–12 weeks old; adults: 10–12 months old) were injected intraperitoneally with methoxy-XO4 (10 mg kg⁻¹ body weight, Tocris, cat. no. 4920). After 3 h, mice were transcardially perfused with ice-cold 1× PBS. Hippocampi were collected, and microglia were isolated by using density gradient separation and prepared as described previously with slight modifications¹⁰. In addition to the microglia surface markers CD11b (1:200, clone M1/70, BioLegend, cat. no. 101212) and CD45 (1:200, clone 30-F11, BioLegend, cat. no. 103106), the following lineage markers were added: anti-CD3 (1:300, clone 17A2, BioLegend, cat. no. 100220), anti-CD19 (1:300, clone 6D5, BioLegend, cat. no. 115520), anti-CD45R (1:300, clone RA3-6B2, BD Biosciences, cat. no. 552772), Ly6C (1:300, clone AL-21, BD Biosciences, cat. no. 560593) and Ly6G (1:300, clone 1A8, BD Biosciences, cat. no. 560601) for 20 min at 4 °C. Percentage and MFI of methoxy-XO4-positive CD11b⁺CD45^{low} microglia were determined by flow cytometry using a FACSCanto II (BD Biosciences) and analyzed with FlowJo software (Tree Star).

RNA isolation from isolated microglia. Grafts were isolated from the cortex of 5xFAD mice 4 weeks after injection. In brief, mice were overdosed through i.p. injection of ketamine and xylazine and transcardially perfused with 10 ml of ice-cold PBS. Brains were immediately isolated and divided coronally at the injection site. The cortical grafts were identified under a stereo-microscope and carefully isolated with a small scalpel; as control, small cortical pieces near the transplant were also isolated. The cortical samples were collected in FACS medium and maintained on ice until further use.

Microglia were isolated and gated as described above. CD11b⁺CD45^{low} microglia were directly sorted by FACS into cell lysis buffer with MoFlo Astrios (Beckman Coulter). Total RNA extraction using Arcturus PicoPure RNA Isolation Kit (Thermo Fisher Scientific, cat. no. KIT0204) was performed according to the manufacturer's protocol.

Bulk RNA-seq from isolated microglia. The SMART-Seq v4 Ultra Low Input RNA Kit for Sequencing (Clontech) was used to generate first-strand cDNA from 300 pg of totalRNA. Double-stranded cDNA was amplified by long-distance PCR (13 cycles) and purified via magnetic bead clean-up. Library preparation was carried out as described in the Illumina Nextera XT Sample Preparation Guide. Next, 150 pg of input cDNA was tagged (tagged and fragmented) by the Nextera XT transposome. The products were purified and amplified via a limited-cycle PCR program to generate multiplexed sequencing libraries. For the PCR step, 1:5 dilutions of index 1 (i7) and index 2 (i5) primers were used. The libraries were quantified using the KAPA Library Quantification Kit—Illumina/ABI Prism User Guide (Roche Sequencing Solutions). Equimolar amounts of each library were sequenced on a NextSeq 500 instrument controlled by the NextSeq Control Software, version 2.2.0, using two High Output Kits (75 cycles) with the dual index, single-read run parameters. Image analysis and base calling were done by the Real Time Analysis Software, version 2.4.11. The resulting BCL files were converted into FASTQ files with the bcl2fastq software, version 2.18.

Library preparation and RNA-seq were performed at the Genomics Core Facility 'KFB - Center of Excellence for Fluorescent Bioanalytics' (University of Regensburg; <http://www.kfb-regensburg.de>).

Differential gene expression analysis. FASTQ files were aligned to the mouse genome (GENCODE M21 genome version and transcriptome annotation) using the STAR aligner (version 2.7.2a)³⁰. Aligned BAM files were processed using featureCounts (version 1.6.2) from the subread package³¹ using standard settings to obtain gene counts.

Differential gene expression analysis was performed using the limma/voomWithQualityWeights pipeline from the R package loom³². Genes were deemed differentially expressed at an adjusted *P* of less than 0.01. For the volcano plot, data were plotted using R packages ggplot2 (version 3.3.3) and ggrepel (version 0.9.1). An expression heat map was generated from the expression data using the R package pheatmap³³.

Microglia depletion. CSF-1R inhibitor BLZ945 (Novartis) was dissolved in 20% (2-hydroxypropyl)-β-cyclodextrin (Sigma-Aldrich). A dose of 200 mg kg⁻¹ body weight was used. In 9–10-week-old *Cx3cr1^{+/+}/5xFAD* mice, BLZ945 was administered by oral gavage for 30 consecutive days starting 3 d before cell transplantation. The mice were killed and analyzed 1 d after the last application.

Organotypic brain slice cultures. Organotypic brain slices from 9–11-month-old *Cx3cr1^{+/+}/5xFAD* and P6–7 WT (C57BL6J) mice were prepared as previously described³⁰. In brief, postnatal WT mice were killed by decapitation and aged mice by CO₂ inhalation, following animal handling laws. After brain isolation, the olfactory bulb, midbrain, brain stem and cerebellum were removed, and the remaining cortical hemispheres were separated and cut sagittally at 350 µm using a tissue chopper (McIlwain, model TC752, Mickle Laboratory Engineering). Intact cortico-hippocampal slices from postnatal brains and cortical slices from aged brains were selected in a pre-cooled dissection medium (50% HEPES-buffered MEM, 1% penicillin–streptomycin, 10 mM Tris, pH 7.2) and incubated in the same medium for 30 min at 4 °C. Two postnatal cortico-hippocampal slices were plated together with two aged cortical slices onto a 0.4-µm porous polytetrafluoroethylene membrane insert (PICMORG50, Millipore) placed in a 3.5-cm dish containing slice culture medium (50% HEPES-buffered MEM, 25% HBSS, 1 mM L-glutamine (Gibco) and 25% heat-inactivated horse serum (Merck-Sigma)). A minimum of nine co-culture dishes were prepared using one aged *Cx3cr1^{+/+}/5xFAD* mouse per experiment (*n* = 2). Medium was exchanged 1 d after preparation and subsequently every 3–4 d. Slices were kept in culture for 2 weeks and then fixed in 4% PFA/sucrose for 15 min at room temperature, followed by three washes with PBS. For the immunohistochemical analysis of co-cultures, slices were permeabilized in PBS containing 0.5% Triton X-100 (PBS-T) for 30 min, cut from the insert using a scalpel and subsequently incubated with the blocking solution (5% NGS in PBS-T) for 1 h at room temperature, followed by overnight incubation at room temperature with the primary anti-GFP antibody (1:500, Fitzgerald, cat. no. 20R-GR011) added to the blocking solution. Slices were washed three times for 10 min with PBS-T and incubated for 3 h at room temperature with blocking solution containing the secondary antibody goat anti-rabbit Alexa Fluor 488 (1:250) (Life Technologies) and Hoechst 33342 for nucleus visualization (1:1,000, cat. no. H3570, Thermo Fisher Scientific). Slices were washed three times for 10 min with PBS-T and subsequently stained with Thiazine Red (Sigma-Aldrich, 2 µM solution in PBS) for 20 min in the dark at room temperature, followed by three PBS-T washing steps. Slices were mounted using Gel Aqua Mount medium (Sigma-Aldrich) and analyzed by confocal microscopy (Leica TCS SP5 II). Representative overview images were acquired with a 10× objective and high-magnification images with a 63× water immersion objective.

Statistical analysis. GraphPad Prism 7 was used for statistical analysis. Student's *t*-test, Mann–Whitney test, Kruskal–Wallis test followed by Dunn's multiple comparison test or one-way or two-way ANOVA followed by Sidak's, Dunn's or Tukey's multiple comparison test was applied. For correlation, the Pearson correlation was used. Reported values are means ± s.e.m. Significance level *α* was set to 0.05; **P* < 0.05, ***P* < 0.01, ****P* < 0.001 and *****P* < 0.0001. No statistical methods were used to predetermine sample sizes, but our sample sizes are similar to those reported in previous publications^{31,32}. Data distribution was assumed to be normal, but this was not formally tested. Investigators were blinded for staining experiments, microglia counts, assessment of Aβ and flow cytometry experiments.

Reporting Summary. Further information on research design is available in the Nature Research Reporting Summary linked to this article.

Data availability

The data that support the findings of this study are available from the corresponding author upon reasonable request. The raw data for RNA sequences of this project are available at the Gene Expression Omnibus under accession code GSE162920. Source data are provided with this paper.

Code availability

The code used to analyze these data are available from the corresponding author upon reasonable request.

References

- Feng, G. et al. Imaging neuronal subsets in transgenic mice expressing multiple spectral variants of GFP. *Neuron* **28**, 41–51 (2000).
- Oakley, H. et al. Intraneuronal β-amyloid aggregates, neurodegeneration, and neuron loss in transgenic mice with five familial Alzheimer's disease mutations: potential factors in amyloid plaque formation. *J. Neurosci.* **26**, 10129–10140 (2006).
- Jung, S. et al. Analysis of fractalkine receptor CX₃CR1 function by targeted deletion and green fluorescent protein reporter gene insertion. *Mol. Cell Biol.* **20**, 4106–4114 (2000).

30. Dobin, A. et al. STAR: ultrafast universal RNA-seq aligner. *Bioinformatics* **29**, 15–21 (2013).
31. Liao, Y., Smyth, G. K. & Shi, W. featureCounts: an efficient general purpose program for assigning sequence reads to genomic features. *Bioinformatics* **30**, 923–930 (2014).
32. Liu, R. et al. Why weight? Modelling sample and observational level variability improves power in RNA-seq analyses. *Nucleic Acids Res.* **43**, e97 (2015).
33. Kolde, R. pheatmap: Pretty heatmaps [Software] (2015).

Acknowledgements

We are particularly grateful to J. Göldner, D. Bleckmann, P. Petry, P. Aktories, J. von Ehr, N. Hagemeyer, T. Masuda, M. Oberle and C. Lange for technical assistance. We also would like to thank J. Zeller for graphical illustrations. Funding: M.M.-L. was supported by the German Research Foundation (ME 3542/2-1) and the Alzheimer Forschung Initiative e.v. (grant no. 18047). V.M.R. and K.J. were funded by the German Federal Ministry of Research and Education (FMT 13GW0230A and MEPHISTO 031L0260B). S.T. is supported by the Alzheimer Forschung Initiative e.v. (grant no. 18014) and the NCL Foundation. M.P. is supported by the Sobek Foundation, the Ernst Jung Foundation, the German Research Foundation (SFB 992, SFB/TRR167, SFB1160, the Reinhart-Koselleck-Grant and the Gottfried Wilhelm Leibniz Prize), the Alzheimer Foundation and the German Research Foundation under Germany's Excellence Strategy (CIBSS – EXC-2189 – Project ID 390939984).

Author contributions

P.d'E., M.P. and M.M.-L. conceived the experiments. P.d'E., S.Z.-W., V.A., P.H., D.E., C.M., S.L., V.M.R., K.J., O. Staszewski, K.K. and O. Schnell performed experiments. P.d'E., S.L. and K.K. contributed to the in vivo imaging studies. L.S.M. and S.T. performed and analyzed slice culture experiments. O. Staszewski analyzed the RNA-seq data. P.d'E., S.Z.-W., O. Staszewski, M.P. and M.M.-L. discussed the results. P.d'E. and M.M.-L. wrote the manuscript. M.M.-L. supervised the project and coordinated the study. All authors edited the paper.

Competing interests

The authors declare no competing interests.

Additional information

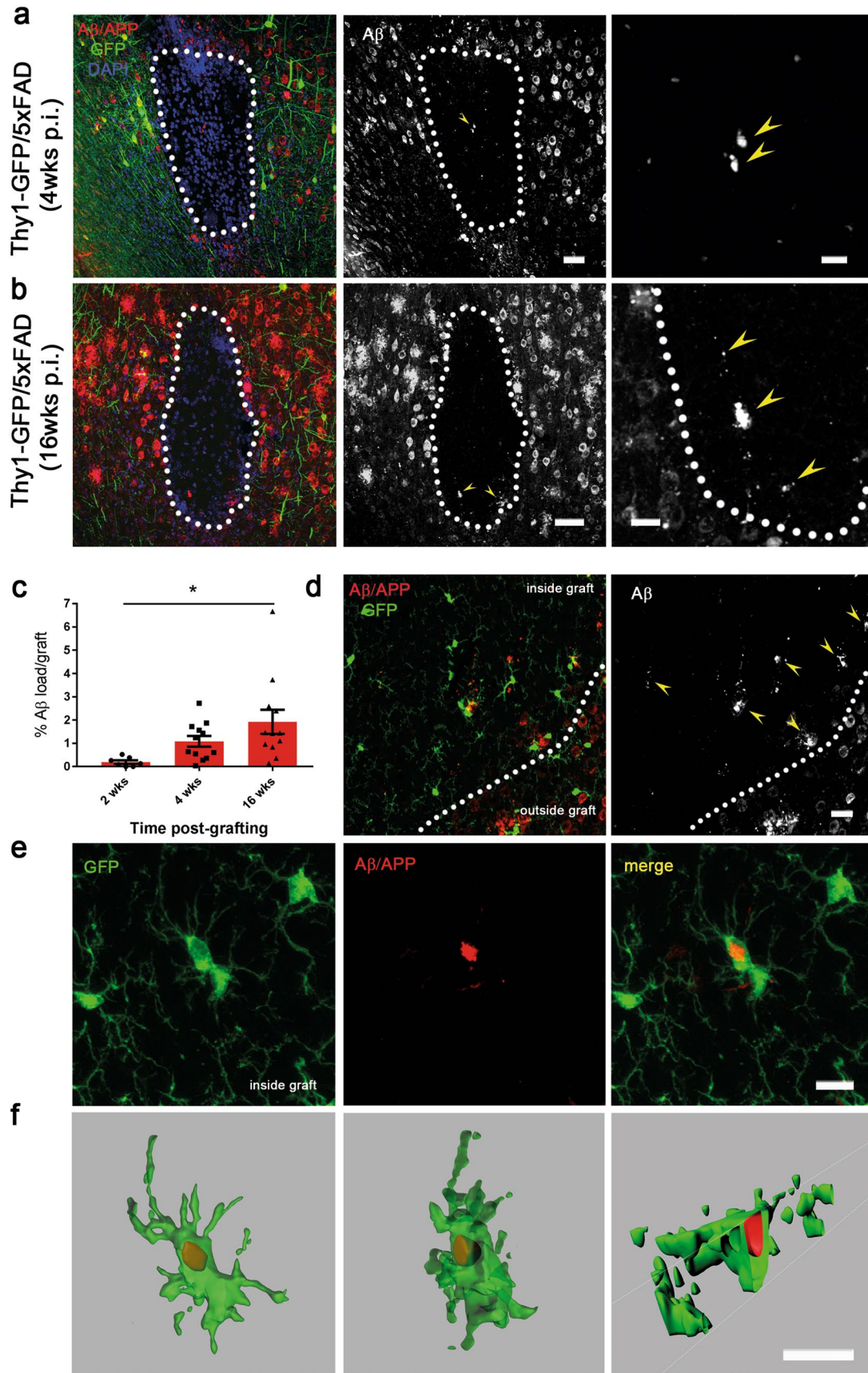
Extended data is available for this paper at <https://doi.org/10.1038/s41593-021-00951-0>.

Supplementary information The online version contains supplementary material available at <https://doi.org/10.1038/s41593-021-00951-0>.

Correspondence and requests for materials should be addressed to Melanie Meyer-Luehmann.

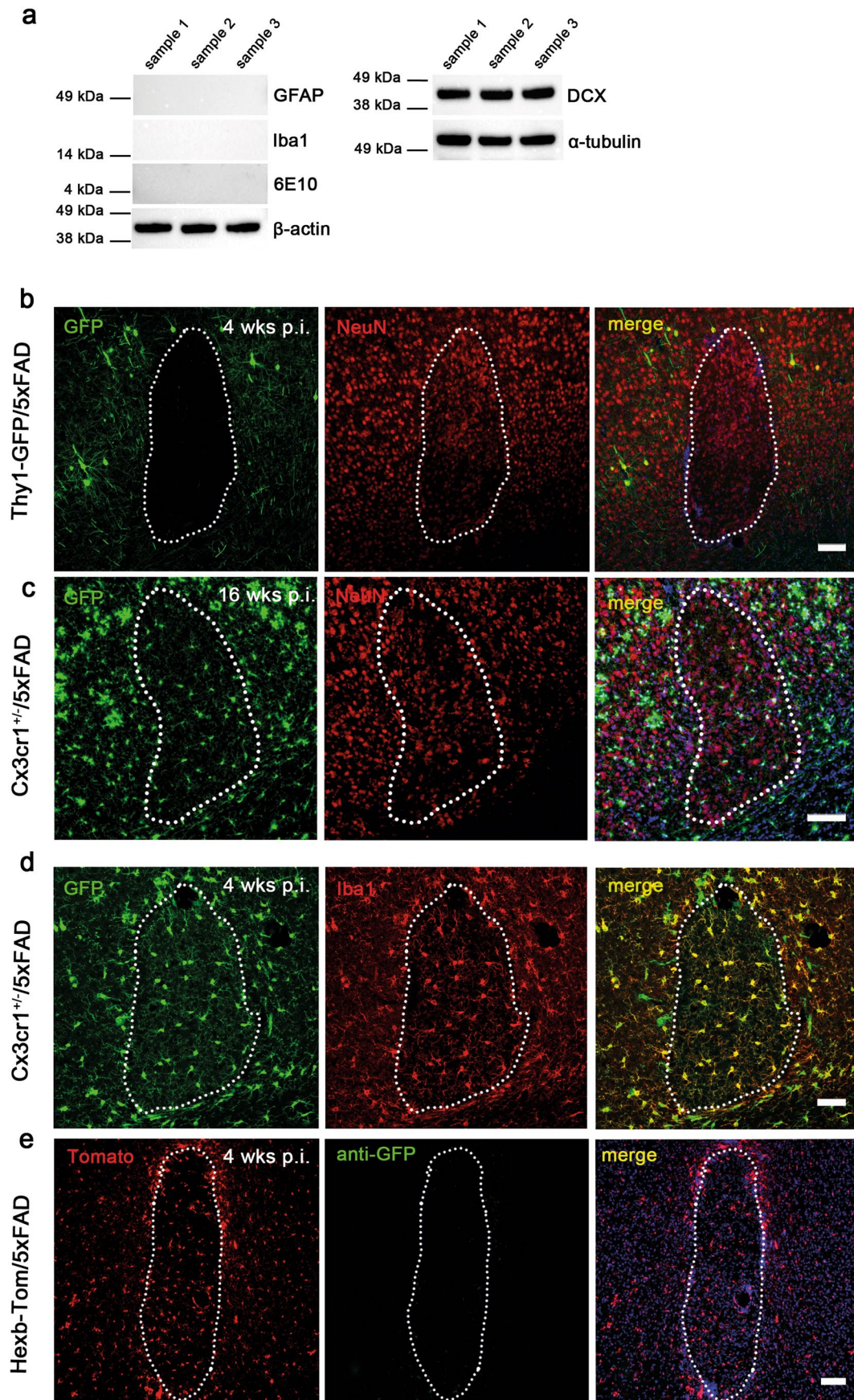
Peer review information *Nature Neuroscience* thanks Srikant Rangaraju and the other, anonymous, reviewer(s) for their contribution to the peer review of this work.

Reprints and permissions information is available at www.nature.com/reprints.



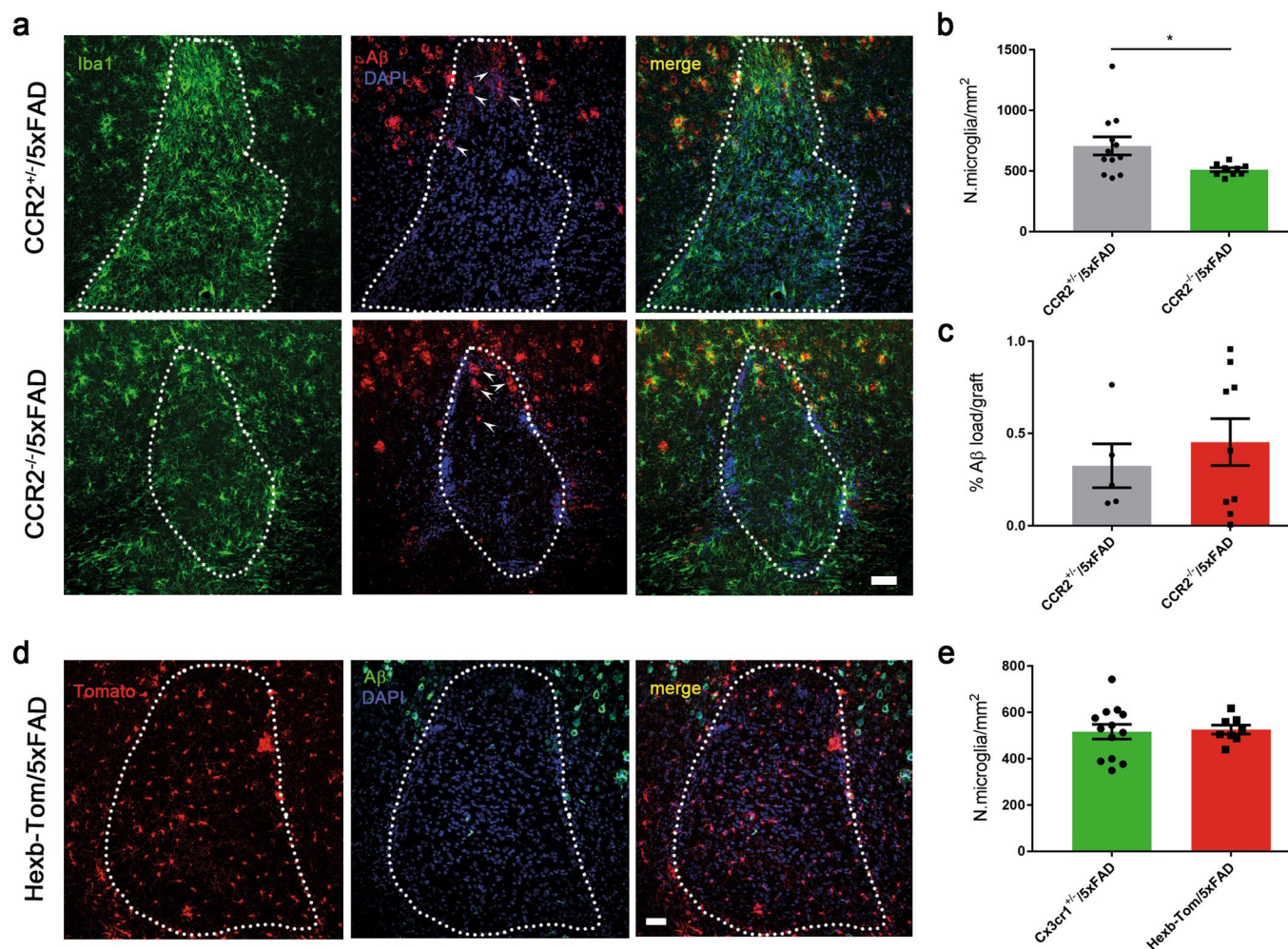
Extended Data Fig. 1 | See next page for caption.

Extended Data Fig. 1 | A β deposits in WT grafts. (a,b) Fluorescence microscopy of grafts in Thy1-GFP/5xFAD recipient mice at (a) 4 weeks p.i. and (b) 16 weeks p.i. immunostained for A β (6E10, red and white; yellow arrowheads indicate the amyloid deposition) and DAPI (blue). Scale bar, 50 μ m in the overview (a) and (b), 20 μ m in the higher magnification (a), 25 μ m in the higher magnification (b). $n = 3$ mice per incubation time. **(c)** Histogram showing the percentage of A β accumulation inside the grafts of Cx3cr1^{+/−}/5xFAD recipient mice at 2, 4 and 16 weeks p.i.. Each symbol represents one graft from $n = 4$ (2 weeks p.i.), $n = 9$ (4 weeks p.i.) and $n = 8$ (16 weeks p.i.) mice. Data are presented as mean (\pm s.e.m.). Significant differences were determined by one-way ANOVA followed by Tukey's multiple comparison test, $F(2, 28) = 4.412$ ($*P = 0.0175$). **(d-f)** Representative confocal microscopy showing (d) A β localization (6E10, red) in the graft and **(e)** high magnification acquisition (f) and Imaris-3D reconstruction of microglia (GFP, green) containing A β (red). Scale bars, 50 μ m in (d), 10 μ m in (e) and (f). $n = 3$ mice.

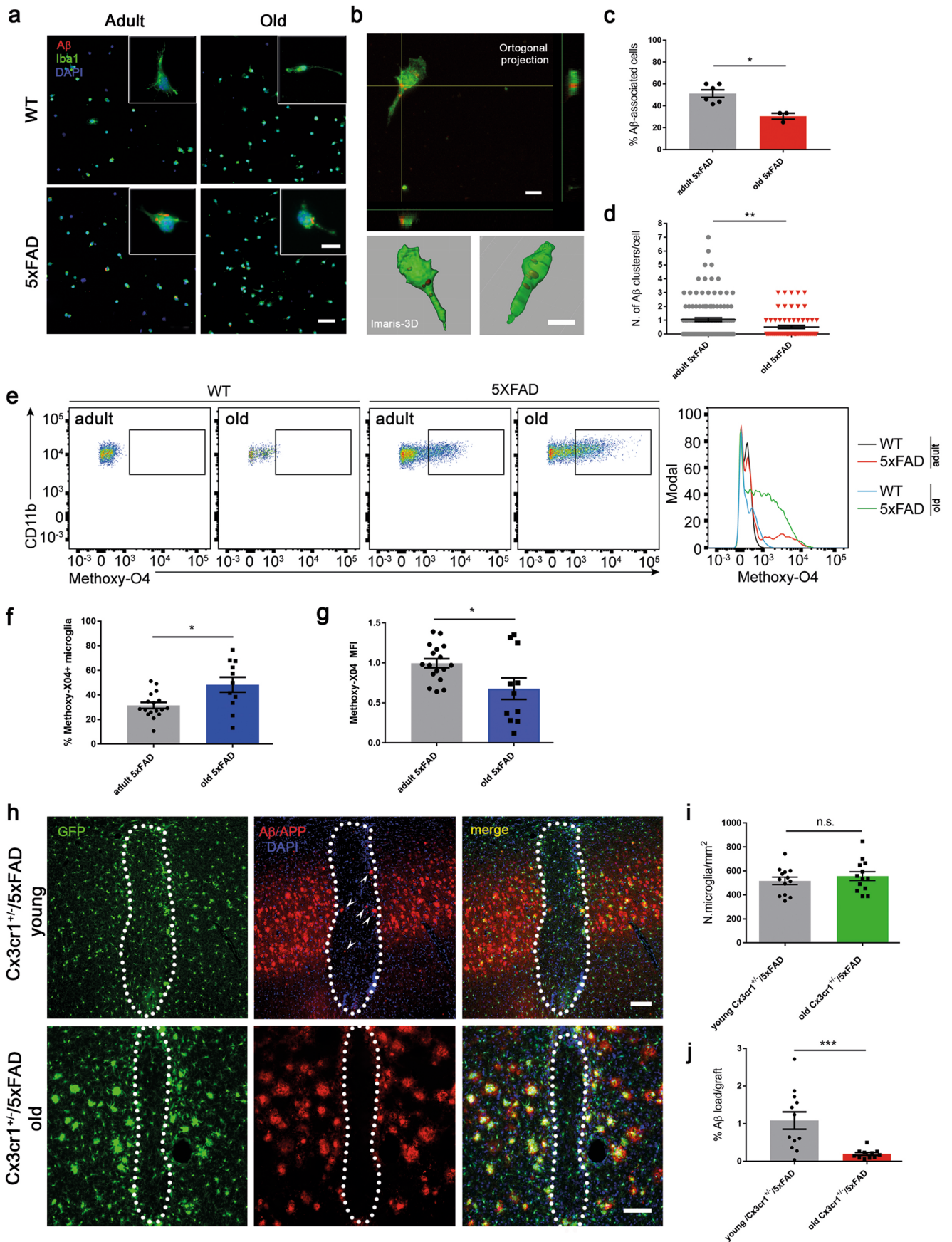


Extended Data Fig. 2 | See next page for caption.

Extended Data Fig. 2 | Cellular composition of cortical WT grafts. **(a)** Immunoblot analysis of cortical cell suspension that were used for grafting experiments. For the blot in the left panel, every protein was detected on separate membranes and only the loading control from the GFAP gel is shown. For uncropped gels with corresponding loading controls see Source Data Extended Data Fig. 2. $n = 3$ independent cell suspensions. **(b)** Representative confocal image of a graft in Thy1-GFP/5xFAD recipient mouse immunostained with NeuN (red) and DAPI (blue). $n = 1$ mouse. **(c)** Representative microscopy of a graft at 16 weeks p.i. of a Cx3cr1^{+/-}/5xFAD recipient mouse immunostained with NeuN (red) and DAPI (blue). $n = 1$ mouse. **(d)** Confocal image of a graft in Cx3cr1^{+/-}/5xFAD recipient mouse immunostained with Iba1 (red). $n = 3$ mice. **(e)** Confocal image of a graft in Hexb-tom/5xFAD recipient mouse transplanted with neurons from Cx3cr1-GFP embryos and counterstained with DAPI (blue). Scale bars 100 μm in (b), (c) and (e), 50 μm in (d). $n = 4$ mice.

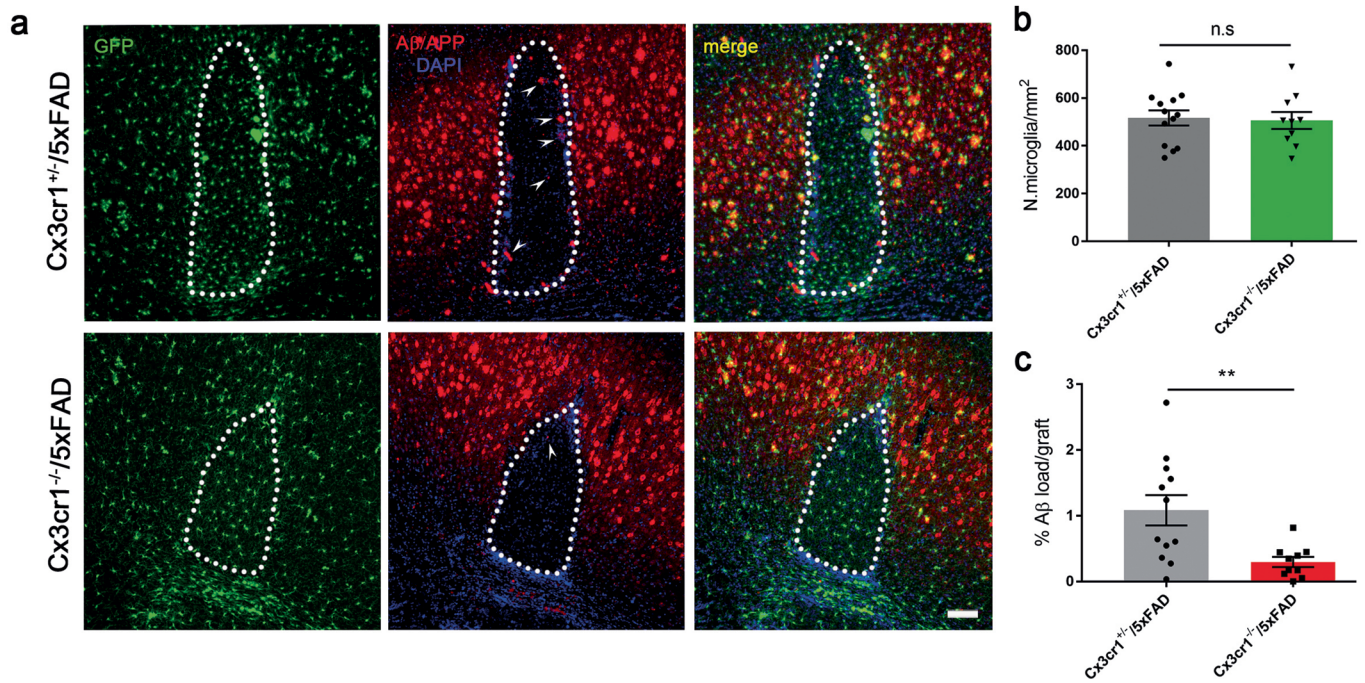


Extended Data Fig. 3 | Resident microglia influence A β accumulation within the grafts. **(a)** Fluorescence microscopy of a graft in CCR2^{+/+}/5xFAD (top) and CCR2^{-/-}/5xFAD (bottom) mice immunostained for A β (6E10, red; white arrowheads indicate the A β), Iba1 (green) and DAPI (blue). Scale bar, 50 μ m. **(b and c)** Graphs show mean (\pm s.e.m.) of **(b)** microglia density and **(c)** percentage of A β inside grafts in the two groups of mice. Each symbol represents one graft from $n=7$ CCR2^{+/+}/5xFAD and $n=4$ CCR2^{-/-}/5xFAD mice. Significant differences were determined by the Mann-Whitney test ($*P=0.04$). **(d)** Fluorescence microscopy of a graft in Hexb-tom/5xFAD recipient immunostained for A β (6E10, green), and DAPI (blue). Scale bar, 50 μ m. **(e)** Histogram compares mean (\pm s.e.m.) of microglia density in grafts of Cx3cr1^{+/+}/5xFAD and Hexb-tom/5xFAD recipient mice. Each symbol represents one graft from $n=8$ Cx3cr1^{+/+}/5xFAD and $n=4$ Hexb-tom/5xFAD. Significant differences were determined by the two-tailed Mann-Whitney test.

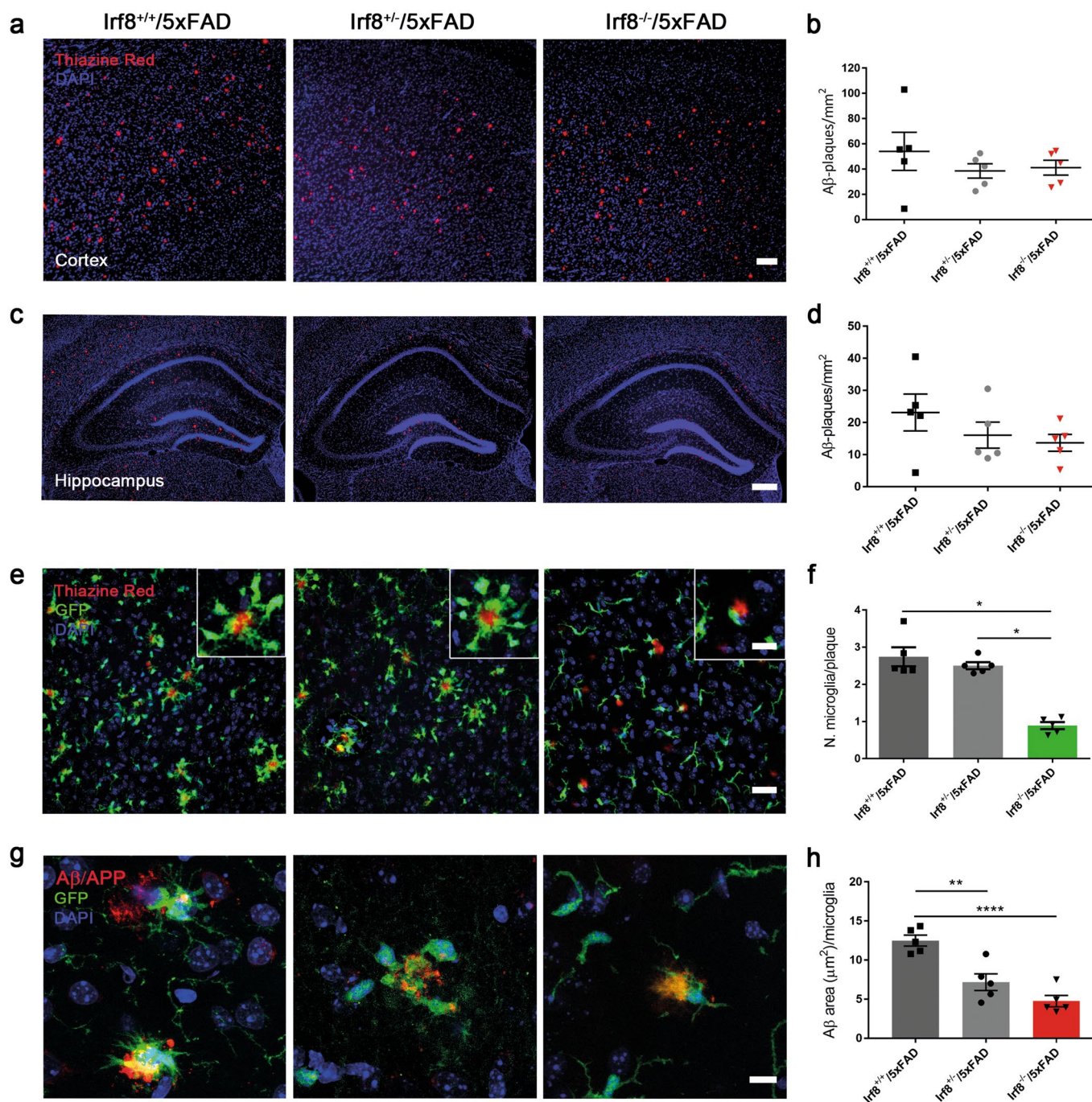


Extended Data Fig. 4 | See next page for caption.

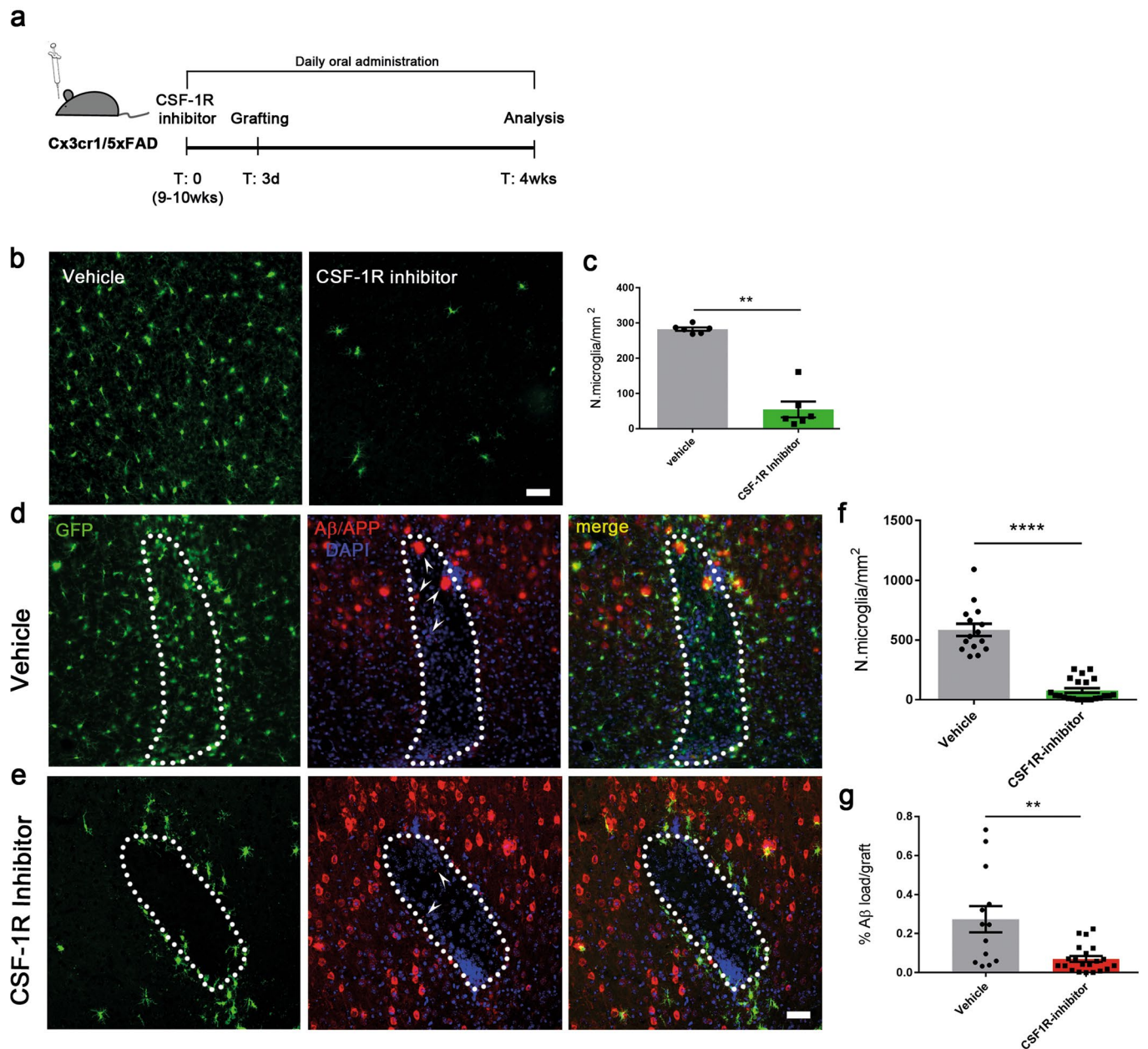
Extended Data Fig. 4 | Less A β deposition inside grafts of adult recipient mice. **(a and b)** Confocal microscopy of microglia cells in vitro isolated from adult (WT and 5xFAD) or old (WT and 5xFAD) mice immunostained for A β (6E10, red), Iba1 (green) and DAPI (blue). Scale bar 50 μ m in the overview and 10 μ m in the inset. **(b)** Confocal orthogonal projection (top) and Imaris-3D reconstruction (bottom) of a single microglia cell containing A β material. Scale bars, 10 μ m. **(c and d)** Graph shows mean (\pm s.e.m.) of A β -associated microglia **(c)** in cells isolated from adult and old 5xFAD mice. Each symbol represents data from one mouse, $n=6$ adult 5xFAD and $n=3$ old 5xFAD mice. Significant differences were determined by the two-tailed Mann-Whitney test ($*P=0.023$). **(d)** Number of A β clusters inside each microglia cell from adult and old 5xFAD mice. Each symbol represents one cell. From $n=5$ adult 5xFAD and $n=3$ old 5xFAD mice. Significant differences were determined by the two-tailed Mann-Whitney test ($***P=0.0038$). **(e-g)** Methoxy-XO4 FACS analysis of microglia isolated from adult and old 5xFAD mice. **(e)** Representative FACS dot-plots (left) and cytometry graph (right) for WT, adult 5xFAD and old 5xFAD mice. Quantification of the **(f)** percentage (%) and **(g)** mean fluorescence intensity (MFI) of methoxy-XO4 positive CD11b⁺CD45^{low} hippocampal microglial cells by flow cytometry isolated from the two 5xFAD groups 3 hours after methoxy-XO4 injection. Each symbol represents data from one mouse, with $n=17$ adult 5xFAD and $n=11$ old 5xFAD mice. Data are presented as mean (\pm s.e.m.). Significant differences were determined by the two-tailed Mann-Whitney test ($*P=0.022$ in f; $*P=0.045$ in g). **(h)** Fluorescence microscopy of grafts in young pre-depositing (top) and old (bottom) Cx3cr1^{+/-}/5xFAD mice immunostained for A β (6E10, red; white arrowheads indicate A β deposition) and DAPI (blue). Scale bar, 100 μ m. **(i and j)** Graphs show mean (\pm s.e.m.) of **(i)** microglia density and **(j)** percentage of A β inside grafts in the two groups of mice. Each symbol represents one graft from $n=9$ young Cx3cr1^{+/-}/5xFAD and $n=7$ old Cx3cr1^{+/-}/5xFAD mice. Significant differences were determined by the two-tailed Mann-Whitney test ($P=0.544$ in i; $***P=0.0005$ in j).



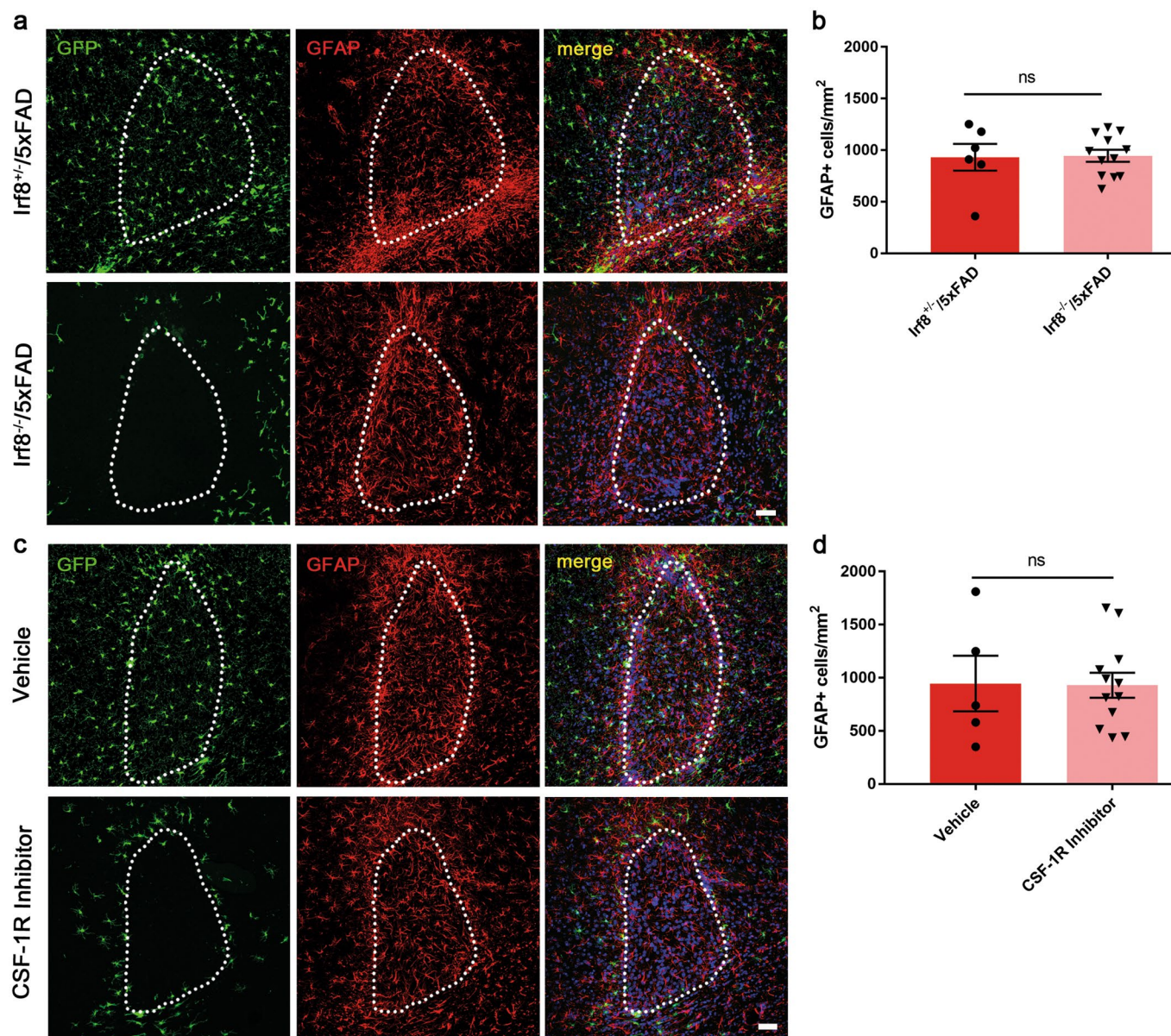
Extended Data Fig. 5 | Reduced A β deposition inside grafts of Cx3cr1^{-/-}/5xFAD recipient mice. (a) Fluorescence microscopy of a graft in Cx3cr1^{+/+}/5xFAD (top) and Cx3cr1^{-/-}/5xFAD (bottom) mice immunostained for A β (6E10, red; white arrowheads indicate A β), and DAPI (blue) at 4 weeks p.i. Scale bar, 100 μ m. **(b and c)** Graphs show mean (\pm s.e.m.) of **(b)** microglia density and **(c)** percentage of A β inside the grafts. Each symbol represents one graft from $n=9$ Cx3cr1^{+/+}/5xFAD and $n=7$ Cx3cr1^{-/-}/5xFAD mice. Significant differences were determined by the two-tailed Mann-Whitney test (** $P=0.009$).



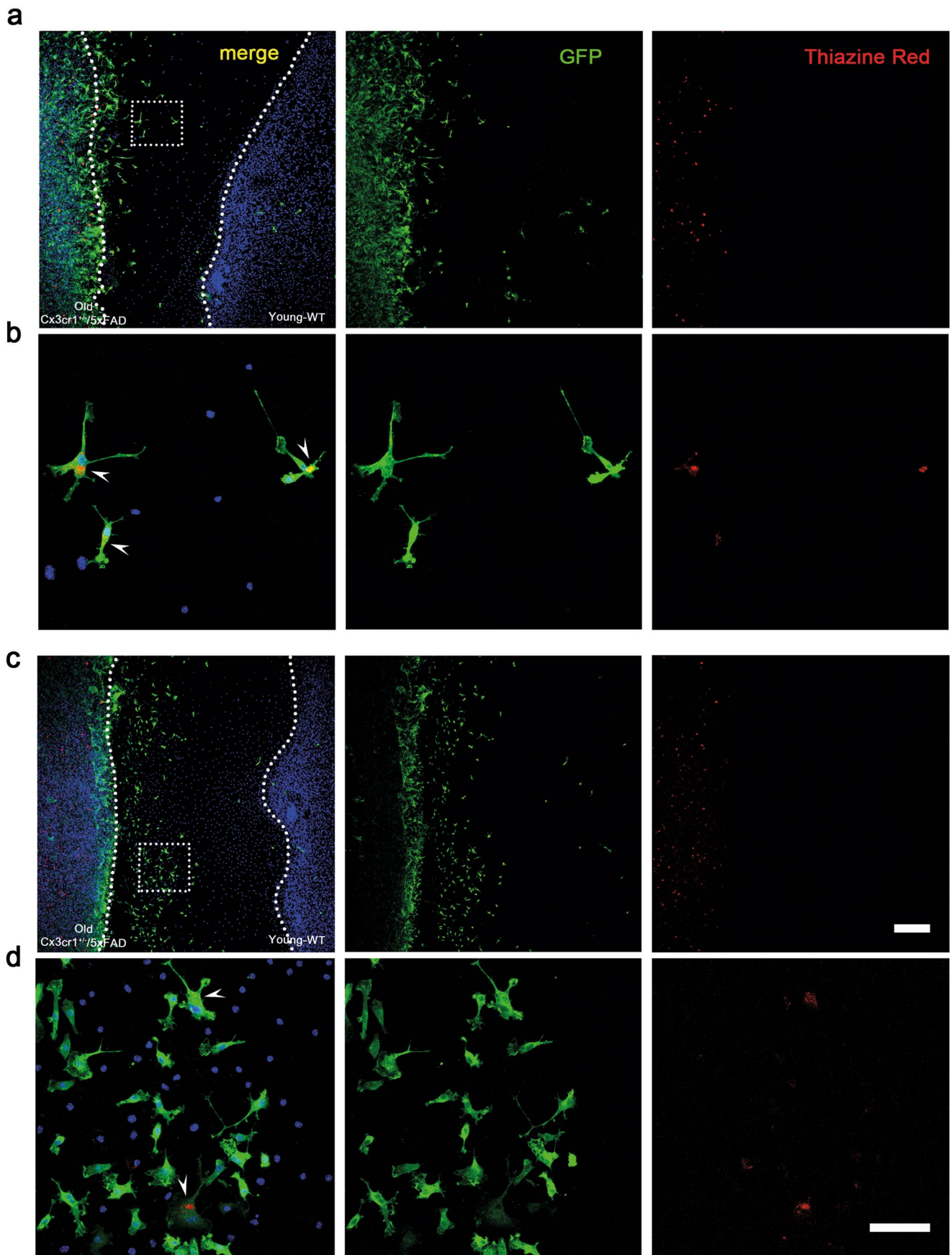
Extended Data Fig. 6 | Quantification of Aβ-plaques in Irf8^{-/-}/Cx3cr1^{+/-}/5xFAD mice. (a,c) Fluorescence microscopy of Irf8^{+/+}/Cx3cr1^{+/-}/5xFAD (left), Irf8^{+/-}/Cx3cr1^{+/-}/5xFAD (middle) and Irf8^{-/-}/Cx3cr1^{+/-}/5xFAD (right) cortices (a) and hippocampi (c) stained with Thiazine Red (red) and DAPI (blue). Scale bar, 100 μm in (a); 300 μm in (c). (b,d) Graphs show the mean (± s.e.m.) of Thiazine Red positive Aβ plaques in the three groups of mice in the cortex (b) and hippocampus (d). Each symbol represents one mouse from n=5 mice per group. Significant differences were determined by one-way ANOVA followed by Tukey's multiple comparison test. (e) Confocal microscopy of Irf8^{+/+}/Cx3cr1^{+/-}/5xFAD (left), Irf8^{+/-}/Cx3cr1^{+/-}/5xFAD (middle) and Irf8^{-/-}/Cx3cr1^{+/-}/5xFAD (right) cortices stained with Thiazine Red (red) and DAPI (blue). Scale bar, 30 μm; inset, 10 μm. (f) Graph shows the mean number (± s.e.m.) of microglia per plaque in the three groups. Each symbol represents one mouse from n=5 mice per genotype. Significant differences were determined by Kruskal-Wallis test followed by Dunn's multiple comparisons test, (*P=0.014; *P=0.04). (g) Confocal microscopy of Irf8^{+/+}/Cx3cr1^{+/-}/5xFAD (left), Irf8^{+/-}/Cx3cr1^{+/-}/5xFAD (middle) and Irf8^{-/-}/Cx3cr1^{+/-}/5xFAD (right) cortices immunolabeled with 6E10 antibody (red) and DAPI (blue). Scale bar, 10 μm. (h) Graph shows the mean (± s.e.m.) of Aβ internalized by microglia in the three groups of mice. Each symbol represents one mouse from n=5 mice per group. Significant differences were determined by one-way ANOVA followed by Tukey's multiple comparison test, F(2, 12) = 21.8 (**P=0.0022; ****P<0.0001).



Extended Data Fig. 7 | Reduced A β deposition inside grafts of microglia-depleted Cx3cr1^{+/-}/5xFAD mice. (a) Experimental setup for the elimination of microglia and transplantation procedure in Cx3cr1^{+/-}/5xFAD mice. (b) Fluorescence microscopy of Cx3cr1^{+/-}/5xFAD cortex treated with vehicle (left) or CSF-1R inhibitor (right). Scale bar, 50 μ m. (c) Quantification shows mean (\pm s.e.m.) of cortical microglia density after treatment. Each symbol represents one mouse of $n = 6$ mice per group. Significant differences were determined by the two-tailed Mann-Whitney test (** $P = 0.0022$). (d-e) Fluorescence microscopy of a graft in Cx3cr1^{+/-}/5xFAD mice treated for 30 days with (d) CSF-1R vehicle or (e) CSF-1R inhibitor and immunostained for A β (6E10, red; white arrowheads indicate A β), and DAPI (blue). Scale bar, 50 μ m. (f and g) Graphs show mean (\pm s.e.m.) of (f) microglia density and (g) percentage of A β inside the graft in the two groups of mice. Each symbol represents one graft from $n = 8$ mice per group. Significant differences were determined by the two-tailed Mann-Whitney test (**** $P < 0.0001$; ** $P = 0.0031$).



Extended Data Fig. 8 | Astrocytes accumulate in grafts of $Irf8^{-/-}/Cx3cr1^{+/+}/5xFAD$ and microglia depleted $Cx3cr1^{+/+}/5xFAD$ mice. (a,c) Confocal image of a graft in (a) $Irf8^{+/+}/Cx3cr1^{+/+}/5xFAD$ (top), $Irf8^{-/-}/Cx3cr1^{+/+}/5xFAD$ (bottom) and (c) $Cx3cr1^{+/+}/5xFAD$ mouse treated with vehicle (top) or with CSF-1R inhibitor (bottom) immunostained with an antibody against GFAP (red) and DAPI (blue). Scale bar, 50 μm . (b,d) Graphs show mean density (\pm s.e.m.) of GFAP-positive astrocytes in (b) $Irf8/Cx3cr1^{+/+}/5xFAD$ and in (d) microglia depleted mice. Each symbol represents one graft from $n = 4$ mice per genotype. Significant differences were determined by the two-tailed Mann-Whitney test.



Extended Data Fig. 9 | See next page for caption.

Extended Data Fig. 9 | Microglia migrate and transport A β from the old Cx3cr1^{+/-}/5xFAD to the young WT brain slices in the co-culture model. (a-d) Confocal images of co-cultures of organotypic brain slices from aged Cx3cr1^{+/-}/5xFAD and postnatal WT mice. Slices were immunolabelled with GFP (green), Thiazine Red (red) and Hoechst (blue). **(a,c)** Overview images of two representative co-cultures. Boxed regions in **(a, c)** are shown with a higher magnification in **(b, d)** and depict migrating 5xFAD microglia (GFP⁺) carrying A β (Thiazine Red⁺) from the aged AD tissue towards the young WT tissue. Scale bars, 200 μ m **(a, c)**, 50 μ m **(b, d)**. n = 9 co-cultured brain slices from n = 2 mice per genotype.

Reporting Summary

Nature Research wishes to improve the reproducibility of the work that we publish. This form provides structure for consistency and transparency in reporting. For further information on Nature Research policies, see [Authors & Referees](#) and the [Editorial Policy Checklist](#).

Statistics

For all statistical analyses, confirm that the following items are present in the figure legend, table legend, main text, or Methods section.

n/a Confirmed

- The exact sample size (n) for each experimental group/condition, given as a discrete number and unit of measurement
- A statement on whether measurements were taken from distinct samples or whether the same sample was measured repeatedly
- The statistical test(s) used AND whether they are one- or two-sided
Only common tests should be described solely by name; describe more complex techniques in the Methods section.
- A description of all covariates tested
- A description of any assumptions or corrections, such as tests of normality and adjustment for multiple comparisons
- A full description of the statistical parameters including central tendency (e.g. means) or other basic estimates (e.g. regression coefficient) AND variation (e.g. standard deviation) or associated estimates of uncertainty (e.g. confidence intervals)
- For null hypothesis testing, the test statistic (e.g. F , t , r) with confidence intervals, effect sizes, degrees of freedom and P value noted
Give P values as exact values whenever suitable.
- For Bayesian analysis, information on the choice of priors and Markov chain Monte Carlo settings
- For hierarchical and complex designs, identification of the appropriate level for tests and full reporting of outcomes
- Estimates of effect sizes (e.g. Cohen's d , Pearson's r), indicating how they were calculated

Our web collection on [statistics for biologists](#) contains articles on many of the points above.

Software and code

Policy information about [availability of computer code](#)

Data collection

Fluorescently labeled brain slices or cell cultures were acquired using a Zeiss fluorescent microscope (Axio Imager M2M) or an Olympus confocal microscope (Fluoview FV 1000). Organotypic brain slices were acquired using a confocal microscopy (Leica TCS SP5 II). In vivo imaging was performed with an Olympus FV1000 two-photon microscope with Mai Tai DeepSee Laser (Spectra-Physics, Newport Corporation, Franklin, MA, USA). 3D reconstruction was performed using IMARIS 8 software. Western blot membranes were visualized with ImageLab 4 software (Bio-Rad Laboratories).

Data analysis

ImageJ 1.52a was used for all immunohistochemical analyses and for quantification of two-photon in vivo acquisitions. The cDNAs libraries for Bulk-RNA sequencing were quantified using the KAPA Library Quantification Kit - Illumina/ABI Prism User Guide (Roche Sequencing Solutions, Inc., Pleasanton, CA, USA) and image analysis done by the Real Time Analysis Software (RTA) v2.4.11. Each library was sequenced on a NextSeq 500 instrument controlled by the NextSeq Control Software (NCS) v2.2.0. The resulting .bcl files were converted into .fastq files with the bcl2fastq v2.18 software.
For the analysis of flow cytometry experiments the FlowJo software (Tree Star) was utilized.
GraphPad Prism 7 (GraphPad Software, Inc) was used for statistical analysis and to generate graphs presented throughout the manuscript.

For manuscripts utilizing custom algorithms or software that are central to the research but not yet described in published literature, software must be made available to editors/reviewers. We strongly encourage code deposition in a community repository (e.g. GitHub). See the Nature Research [guidelines for submitting code & software](#) for further information.

Data

Policy information about [availability of data](#)

All manuscripts must include a [data availability statement](#). This statement should provide the following information, where applicable:

- Accession codes, unique identifiers, or web links for publicly available datasets
- A list of figures that have associated raw data
- A description of any restrictions on data availability

All relevant data are available from the authors upon request.

Field-specific reporting

Please select the one below that is the best fit for your research. If you are not sure, read the appropriate sections before making your selection.

Life sciences Behavioural & social sciences Ecological, evolutionary & environmental sciences

For a reference copy of the document with all sections, see [nature.com/documents/nr-reporting-summary-flat.pdf](https://www.nature.com/documents/nr-reporting-summary-flat.pdf)

Life sciences study design

All studies must disclose on these points even when the disclosure is negative.

Sample size	Sample size was determined based on experience from previous studies (Meyer-Luehmann et al. Nature Neuroscience 2003; Meyer-Luehmann et al. Nature 2008), including the success rate of intracerebral grafting and two-photon imaging.
Data exclusions	Data were excluded if intracerebral grafting was unsuccessful and no graft was present; The number of mice per genotype were excluded as follows: 5xFAD/Cx3cr1+/-=5; 5xFAD/Cx3cr1-/-=3; old recipients 5xFAD/Cx3cr1+/-=4; 5xFAD/Irf8+/-=1; 5xFAD/CCR2+/-=3; 5xFAD/CCR2-/-=3.
Replication	All attempts of replication were successful. To analyze A β inside primary microglia, between 20 and 50 cells per mouse were quantified and replicated on at least 3 mice per group. The western blot analysis of freshly isolated cortical cells for grafting were performed on three independent preparations. Methoxy-XO4 FACS analysis of microglia isolated from young-adult and aged 5xFAD mice was performed in three repeated experiments using at least 3 mice per group in each experiment. For the Bulk-RNA sequencing, graft and control cortical region isolation was repeated three times and for each independent experiment 7-10 mice were used. The grafting experiments were repeated at least three times using, when possible, at least 2 mice per group per experiments. The organotypic brain slice experiments were replicated two times using one mouse per group in each experiment. The in vivo laser lesion experiments were performed in at least 4 repeated experiments per animal group using one mouse in each experiment.
Randomization	For all experiments, mice were randomly allocated into each experimental group by PdE and CM.
Blinding	The investigator was not blinded during the intracerebral grafting experiments since the procedure was independently identical. The investigator was not blinded during two-photon imaging and analysis due to obvious differences in microglia morphology between groups/genotypes. The investigator was blinded for staining experiments, microglia counts and assessment of A β (slides and in vitro samples were imaged and saved with random numbers to identify them) and flow cytometry experiments. Images were then quantified and unblinded to perform group statistics.

Reporting for specific materials, systems and methods

We require information from authors about some types of materials, experimental systems and methods used in many studies. Here, indicate whether each material, system or method listed is relevant to your study. If you are not sure if a list item applies to your research, read the appropriate section before selecting a response.

Materials & experimental systems

n/a	Involved in the study
<input type="checkbox"/>	<input checked="" type="checkbox"/> Antibodies
<input checked="" type="checkbox"/>	<input type="checkbox"/> Eukaryotic cell lines
<input checked="" type="checkbox"/>	<input type="checkbox"/> Palaeontology
<input type="checkbox"/>	<input checked="" type="checkbox"/> Animals and other organisms
<input checked="" type="checkbox"/>	<input type="checkbox"/> Human research participants
<input checked="" type="checkbox"/>	<input type="checkbox"/> Clinical data

Methods

n/a	Involved in the study
<input checked="" type="checkbox"/>	<input type="checkbox"/> ChIP-seq
<input type="checkbox"/>	<input checked="" type="checkbox"/> Flow cytometry
<input checked="" type="checkbox"/>	<input type="checkbox"/> MRI-based neuroimaging

Antibodies

Antibodies used

clone GA5, Sigma-Aldrich #G3893, lot.3140011; anti-GFAP Dako #Z033401-2, lot.00087879; anti-A β clone 6E10 BioLegend #803001-Previously Covance catalog# SIG-39320, lot.B291304; DCX Abcam #ab18723, lot.GR324493-1; α -tubulin Abcam #ab89984, lot.GR3281114-3; β -actin-HRP Abcam #ab20272, lot.GR3256256-1; CD11b-APC, clone M1/70, Biolegend #101212, lot.1912131; anti-GFP, Fitzgerald, cat.no. 20R-GR011; CD45-PE, clone 30-F11, Biolegend #103106, lot.4348413; anti-CD3-PE/Cy7, clone 17A2, Biolegend #100220, lot.B266245; CD19-PE/Cy7, clone 6D5, Biolegend, #115520, lot.B290857; CD45R/B220-PE/Cy7, clone RA3-6B2, BD Bioscience #552772, lot.2008222; Ly6C-PE/Cy7, clone AL-21, BD Bioscience #560593, lot.9080848; Ly6G-PE/Cy7, clone 1A8, BD Bioscience, #560601, lot.8164873, Fixable Viability Dye eFluor[®] 780, eBioscience #65086514, lot.2114524.

Validation

All antibodies used in this study were commercially available and validated by the vendors and previous studies performed by our laboratory or by others.

Animals and other organisms

Policy information about [studies involving animals](#); [ARRIVE guidelines](#) recommended for reporting animal research

Laboratory animals

Grafting experiments:

9-10 weeks or 8-11 months female mus musculus 5xFAD (APP K670N/M671L (Sw)+I716V (Fl)+V717I(Lo) and PS1M146L+L286V) crossed with Cx3cr1+/- in order to obtain Cx3cr1+/-/5xFAD or Cx3cr1-/-/5xFAD; 9-10 weeks female Hexb-tdTomato/5xFAD; Thy1-eGFP/5xFAD; Irf8+/-/Cx3cr1+/-/5xFAD, Irf8+/-/Cx3cr1+/-/5xFAD or Irf8-/-/Cx3cr1+/-/5xFAD; CCR2+/-/5xFAD or CCR2-/-/5xFAD. All mice were maintained on a C57BL/6N background.

Cortical suspension were prepared from WT C57BL/6N embryos (E16-E17). All embryos were used.

Microglia isolation experiments:

Microglia were isolated from 20-30 weeks or 50-60 weeks 5xFAD mice and aged matched C57BL/6N WT controls. Both males and females were used for these experiments.

Laser lesion and in vivo imaging of microglia process outgrowth:

12-14 weeks old female Irf8+/-/Cx3cr1+/-, Irf8+/-/Cx3cr1+/- and Irf8-/-/Cx3cr1+/- mice.

Laser lesion and in vivo imaging of A β -containing microglia in Cx3cr1+/-/5xFAD and Irf8-/-/Cx3cr1+/-/5xFAD mice:

7-10 months old female Cx3cr1+/-/5xFAD and Irf8-/-/Cx3cr1+/-/5xFAD mice.

Organotypic slice co-cultures:

9 months old Cx3cr1+/-/5xFAD and 6days old C57BL/6N WT mice.

Wild animals

No wild animals were used in the study.

Field-collected samples

No field-collected samples were used in the study.

Ethics oversight

All animal experiments were carried out in accordance with the policies of the state of Baden-Württemberg under license number G16-100.

Note that full information on the approval of the study protocol must also be provided in the manuscript.

Flow Cytometry

Plots

Confirm that:

- The axis labels state the marker and fluorochrome used (e.g. CD4-FITC).
- The axis scales are clearly visible. Include numbers along axes only for bottom left plot of group (a 'group' is an analysis of identical markers).
- All plots are contour plots with outliers or pseudocolor plots.
- A numerical value for number of cells or percentage (with statistics) is provided.

Methodology

Sample preparation

Mice were injected intraperitoneally with methoxy-XO4 (Tocris Bioscience; #4920; 10mg/kg bodyweight). Upon 3 hours incubation, mice were transcardially perfused with PBS. Hippocampi were collected and homogenized with a glass potter in HBSS containing 15 mM HEPES buffer and 0.54 % Glucose. Hippocampal brain homogenate was separated by 70/37/30 % layered Percoll gradient centrifugation at 800 g for 30 min at 4 °C (without brake). Subsequently, cell pellet was collected and washed once with PBS before staining. Cells were incubated with Fc receptor blocking antibody CD16/CD32 (2.4G2, BD Bioscience) to prevent unspecific binding and dead cells were stained using the Fixable Viability Dye eFluor[®] 780 (eBioscience) for 10min at 4°C. Cells were stained with primary antibodies directed against CD11b-APC (M1/70, BioLegend), CD45-PE (30-F11, BioLegend, Lineage markers: anti-CD3-PE/Cy7 (17A2, BioLegend), anti-CD19-PE/Cy7 (6D5, BioLegend), anti-CD45R-PE/Cy7 (RA3-6B2, BD Bioscience), Ly6C-PE/Cy7 (AL-21, BD Bioscience), Ly6G-PE/Cy7 (1A8, BD Bioscience) for 20min at 4°C.

Instrument

FACS Canto II (BD Bioscience)

Software

Data were acquired with BD FACSDiva™ SOFTWARE (Becton Dickinson). Post-acquisition analysis was performed using FlowJo software, version X.0.7.

Cell population abundance

Gating on live CD11b+CD45loDUMP- cells results in >95% pure microglial populations, while blood-derived cells and CAMs are excluded.

Gating strategy

The gating strategy for mouse brain samples we used in this study is provided in Supplementary Fig.4. CNS cells were gated for singlets, followed by gating for living cells (Fixable Viability Dye), lineage-negative cells (Dump), CD11b+CD45+ cells and methoxy-O4+ CD11b+CD45+ cells.

Tick this box to confirm that a figure exemplifying the gating strategy is provided in the Supplementary Information.